LUND UNIVERSITY

Mixed Block Copolymer Solutions: Self-Assembly and Interactions

Bayati, Solmaz

2016

[Link to publication](#)

Mixed Block Copolymer Solutions: Self-Assembly and Interactions

PHYSICAL CHEMISTRY | LUND UNIVERSITY
SOLMAZ BAYATI

Mixed Block Copolymer Solutions: Self-Assembly and Interactions

Solmaz Bayati

LUND
UNIVERSITY

DOCTORAL DISSERTATION

by due permission of the Faculty Science, Lund University, Sweden.

To be defended on June 15th, 2016 at 10:30 AM at lecture hall B,

Center for Chemistry and Chemical Engineering, Lund.

Faculty opponent

Prof. Kell Mortensen
Niels Bohr Institute, University of Copenhagen, Denmark

Organization:	Document name:
LUND UNIVERSITY Division of Physical Chemistry P.O. Box 124 221 00 Lund, Sweden	DOCTORAL DISSERTATION
	Date of issue: 2016-06-15
Author: Solmaz Bayati	Sponsoring organization: The Swedish Research Council (VR) The Linnaeus Grant ''Organizing Molecular Matter'' through VR

Title and subtitle:

Mixed Block Copolymer Solutions: Self-Assembly and Interactions

Abstract

This thesis incorporates studies on the aqueous systems of two types of thermoresponsive amphiphilic block copolymers; a series of nonionic triblock copolymers comprising blocks of poly(ethylene oxide) (PEO) and poly(propylene oxide) (PPO) denoted as PEO-PPO-PEO block copolymers, and a series of ionic diblock copolymers consisting of one charged block and one block of poly(N-isopropylacrylamide) (PNIPAAM). Various techniques, such as dynamic and static light scattering (DLS and SLS), small angle X-ray and neutron scattering (SAXS and SANS), high sensitivity differential scanning calorimetry (HSDSC), turbidimetry, electrophoretic mobility measurements, and two-dimensional proton NMR nuclear Overhauser effect spectroscopy (2D ^{1}H NMR NOESY), were applied to study these block copolymer systems.

In the first part of the thesis, the influence of a bile salt, sodium glycodeoxycholate (NaGDC), on the self-assembly of the three PEO-PPO-PEO block copolymers, P123, F127 and P65, was studied. Apart from the fundamental physio-chemical point of view, the overall aim of this study was to investigate if these types of block copolymers are potential candidates to be used as bile acid sequestrants in the treatment of *bile acid diarrhea* and *hypercholesterolemia* diseases. It was found that the NaGDC does influence the self-assembly of these block copolymers in a similar way, but not as effectively as the classical ionic surfactants. At low bile salt concentrations and above the CMT of the pure aqueous solutions of these polymers, charged PEO-PPO-PEO micelle-NaGDC complexes are formed. The SAXS results indicated that the NaGDC molecules are located mostly in the corona of the block copolymer micelles, close to the core-corona interface. However, at higher bile salt concentrations, during their disintegration, these complexes are generally in coexistence with small NaGDC-rich complexes. The latter complexes resemble the NaGDC micelles in terms of size and structure. Among the three studied block copolymers, P65 micelles are the easiest to disintegrate by NaGDC. The F127 and P123 micelles show almost the same stability when interacting with NaGDC.

The second part in this thesis primarily describes the investigation of the effects of temperature, salt, PNIPAAM block length, and polymer concentration on the association behavior of a series of the three diblock copolymers, poly(N-isopropylacrylamide)-b-poly((3-acrylamidopropyl) trimethylammonium chloride) (PNIPAAM$_n$-b-PAMPTMA(+)$_{20}$), where n=24, 48, and 65. It was shown that the cloud point (CP) of the polymer solutions decreases upon an increase in PNIPAAM block length, and polymer and salt concentrations. At temperatures below CP of the polymer solutions, unimers and micellar/intermicellar clusters coexist. However, at temperatures above the CP, the dominant particles in the solutions are the large aggregates, which generally retain stable sizes in the presence of salt and upon increasing the temperature.

Finally the aqueous mixed solutions of PNIPAAM$_{26}$-b-PAMPTMA(+)$_{15}$ and poly(N-isopropylacrylamide)-b-poly(sodium 2-acrylamido-2-methyl-1-propanesulfonate) (PNIPAAM$_{27}$-b-PAMPS($-$)$_{15}$) with an equimolar charge condition were studied. Mixed micelles were observed at total concentrations ranging from 0.2 to 0.5 wt % in all studied temperatures (10– 30 ^{o}C). The mixed micelles have a cylindrical structure, and are formed via an attractive electrostatic interaction between the oppositely charged PAMPTMA(+) and PAMPS($-$) blocks. However, in addition to the charged blocks interaction, there is evidence of interaction between the PNIPAAM and the charged blocks, as demonstrated by 2D ^{1}H NMR NOESY experiments.

Key words:

Polymer, Block Copolymer, PEO-PPO-PEO, Pluronics$^©$, Bile Salt, NaGDC, PNIPAAM, PAMPTMA, PAMPS, Mixed Micelle, Self-Assembly, Mixed Complexes

Classification system and/or index terms (if any)

Supplementary bibliographical information	Language: English

ISSN and key title:	ISBN: 978-91-7422-450-4 (print) 978-91-7422-459-7 (pdf)

Recipient's notes	Number of pages:222	Price
	Security classification	

Signature _Solmaz Bayati_   Date: 2016-05-09

Mixed Block Copolymer Solutions: Self-Assembly and Interactions

Solmaz Bayati

LUND
UNIVERSITY

Contents

Acknowledgments

The 4 year and half of my PhD at Lund University was full of great moments, interesting experiences, meeting wonderful people from all over the world, getting to know lovely friends and learning new things. There are many people whom without their help, I wouldn't have such a feeling today:

Karin Schillén, my dear supervisor, I am honored and deeply pleased that I did my PhD with you. I cannot imagine doing this thesis without your priceless help. Apart from being a great scientist, you are a wonderful person that I learned a lot from. Thanks for being always present to support and encourage whenever and for whatever I needed. I am grateful that you were always taking my scientific and non-scientific questions seriously and answering them all patiently and kindly. I enjoyed every and each moment of travelling with you for the conferences and beam times and all the nice out of work moments we shared together. Words cannot express how grateful I am for all you have done for me. I can just say that to me, you are beyond a supervisor; you are a close friend and a companion.

Tommy Nylander, my co-supervisor, although the change in the scientific path of my PhD thesis, did not allow us to collaborate more, I appreciate your kindness, support and encouragement during my PhD years.

Luciano Galantini, the extent of aid and cooperation that I got from you during the last years of my PhD were limitless and beyond what a collaborator does. Hence, I would like to call you my co-supervisor. Thanks for always being responsible, and available for the fruitful scientific discussions, and sharing your valuable ideas and solutions to improve my PhD project. You were always a kind friend to me and I will never forget the *intro* song of our scientific discussions which was always an energy boost in the difficult moments.

Thanks to ***all my coauthors***, without your valuable scientific inputs, writing of this thesis wouldn't be possible.

2

Popular Science Summary

Polymers are giant molecules consisting of a repetition of many small units (monomers) that are linked together by chemical bonds. If we consider a long necklace as a polymer chain, the beads are the monomers and the part of the thread which connects the beads together is the chemical bond. Polymers are important materials in our everyday life and they can be found e.g., in plastics, paints, fabrics, papers, food materials, cosmetics and drugs.

When a polymer is composed of more than one type of monomer, it is called a copolymer. Copolymers can have a variety of structures depending on how the different monomers are arranged in the polymer chain. One type of these copolymers is called block copolymers. For instance, if we attach the necklace with the pink beads (block A) to the end of the other necklace with the blue beads (block B), then this is called an A-B block copolymer or generally a ''diblock'' copolymer. One can make A-B-A or A-B-C which are called ''triblock copolymers'' or even block copolymers with more than three blocks.

Some of these block copolymers show interesting behavior when they are in contact with water. For instance, they may have a block that hates to be in contact with water (necklace with the red beads) and the other block which loves water (necklace with the blue beads). These types of block copolymers are scientifically called ''amphiphilic'' block copolymers and they are considered polymeric surfactants. To have a favorable condition in water for both blocks, block copolymer chains may arrange themselves in a type of spherical structure that is called a ''micelle''. In this micelle, the blocks which hate water, occupy the core to have less contact with water and the blocks which love water form the corona of the micelle. This spontaneous behavior of the amphiphilic block copolymers in water is called ''self-assembly'' which happens above a specific polymer concentration. Some block copolymers are sensitive to a change in temperature, and hence, temperature can influence their self-assembly. These types of block copolymers are called ''thermoresponsive'' block copolymers. Thus, they self-assemble or form micelles above a specific temperature.
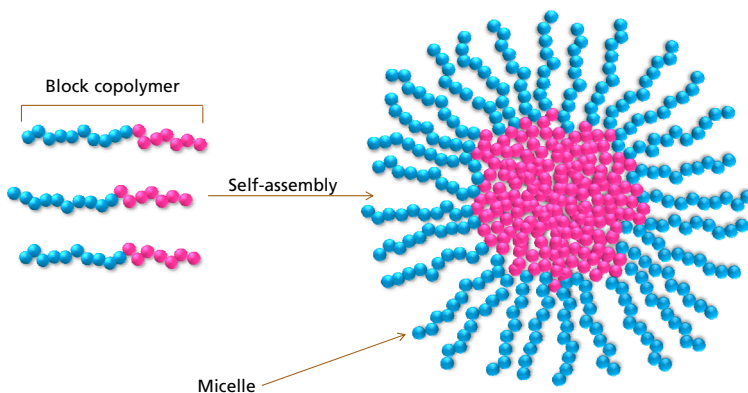
Figure 1. Schematic illustration of the amphiphilic block copolymer and its self-assembly in water to form a micelle.

Micelles of block copolymers play an important role in treatment of some specific diseases. These micelles, with sizes of about several tens of nanometers, can incorporate drug molecules and act as their carriers into the body. Due to their specific structure and the optimal size, they will not be removed from the blood stream and hence, the circulation time of the drug in the body could be increased. The physical and chemical characteristics of the block copolymer micelle can be tuned in a way that makes it suitable for targeting specific organs or tissues in the body to release the drug. Therefore it is very important to study the physical and chemical properties of the block copolymers and their self-assembly behavior. Meaning, for instance studying how different stimuli such as temperature, addition of acid, salt and other types of chemicals can effect on the self-assembly of these block copolymers.

This thesis contains studies on some of the amphiphilic and thermoresponsive diblock and triblock copolymers. Some of these block copolymers have already been used in pharmaceutical applications and some may have the potential to be used.

In this thesis it was demonstrated how block copolymer concentration, temperature, addition of salt and a natural body surfactant (bile salt) as well as the length of the loving-water or the hating-water blocks can influence the self-assembly of the micelles and break them up. Various techniques have been applied to study these block copolymer systems. Results demonstrated that some of these block copolymers could be potential candidates in the treatment of specific diseases for instance, *hypercholesterolemia*.

List of Papers and

Author Contributions

I. Bayati, S., Galantini, L., Knudsen, K. D., Schillén, K., **Effects of Bile Salt Sodium Glycodeoxycholate on the Self-Assembly of PEO–PPO–PEO Triblock Copolymer P123 in Aqueous Solution**, *Langmuir* **2015**, *31*, 13519-13527.

The Author performed all experiments and data analysis. The Author wrote the first draft of the paper.

II. Bayati, S., Galantini, L., Knudsen, K. D., Schillén, K., **Complexes of PEO-PPO-PEO Triblock Copolymer P123 and Bile Salt Sodium Glycodeoxycholate in Aqueous Solution: A Small Angle X-ray and Neutron Scattering Investigation**, *Colloids Surf., A, Under revision.*

The Author performed all SAXS experiments. The SANS experiments were performed together with K. D. Knudsen. The Author analyzed all data and wrote the manuscript together with the co-authors.

III. Bayati, S., Haglund Anderberg, C., Pavel, N., V., Galantini, L., Schillén, K., **Interaction between Bile Salt Sodium Glycodeoxycholate and PEO-PPO-PEO Triblock Copolymers in Aqueous Solution**, *Submitted.*

The Author performed the majority of the experiments and data analysis. The Author wrote the manuscript together with the co-authors.

IV. Bayati, S., Zhu, K., Trinh, L. T., Kjøniksen, A.-L., Nyström, B., **Effects of Temperature and Salt Addition on the Association Behavior of Charged Amphiphilic Diblock Copolymers in Aqueous Solution**, *J. Phys. Chem. B* **2012**, *116*, 11386-11395.

The Author performed all experiments and data analysis except for the asymmetric flow field-flow fractionation experiments that were performed by A.-L. Kjøniksen. K. Zhu synthesized the polymers. The Author wrote the first draft of the paper.

V. Bayati, S., Zhu, K., Nyström, B., Bergquist, K.-E., Pedersen, J. S., Galantini, L., Schillén, K., **Mixed Micelles of Oppositely Charged PNIPAAM Diblock Copolymers**, *Manuscript.*

The Author performed all experiments and data analysis except for the 2D ^{1}H NMR NOESY experiments that were performed by K.-E. Bergquist. K. Zhu synthesized the polymers. The Author wrote the manuscript together with the co-authors.

Papers Not Included in the Thesis

I. Janiak, J., Bayati, S., Galantini, L., Pavel, N. V., Schillén, K., **Nanoparticles with a Bicontinuous Cubic Internal Structure Formed by Cationic and Non-ionic Surfactants and an Anionic Polyelectrolyte**, *Langmuir* **2012**, *28*, 16536-16546.

II. Bayati, S., Pamies, R., Volden, S., Zhu, K., Kjøniksen, A.-L., Glomm, W. R., Nyström, B. **Influence of Poly(ethylene glycol) Block Length on the Adsorption of Thermoresponsive Copolymers onto Gold Surfaces**, *J., Matter Sci.*, **2013**, *48*, 7055-7062.

III. Travaglini, L., Gubitosi, M., di Gregorio, M. C. Pavel, N. V., D'Annibale, A., Giustini, M., Tellini, V. H. S., Tato, J. V., Obiols-Rabasa, M., Bayati, S., Galantini, L. **On the Self-Assembly of a Tryptophan Labeled Deoxycholic acid.** *Phys. Chem. Chem. Phys.* **2014,** *16*, 19492-19504.

List of Abbreviations

NaGDC	Sodium Glycodeoxycholate
PEO	Poly(ethylene oxide)
PPO	Poly(propylene oxide)
PEO-PPO-PEO	Poly(ethylene oxide)-*b*-poly(propylene oxide)-*b*-poly(ethylene oxide)
PNIPAAM	Poly(*N*-isopropylacrylamide)
EO	Ethylene oxide
PO	Propylene oxide
CMT	Critical Micelle Temperature
CMC	Critical Micelle Concentration
SDS	Sodium Dodecyl Sulfate
CTAC	Cetyltrimethyl Ammonium Chloride
LCST	Lower Critical Solution Temperature
CP	Cloud Point
HSDSC	High Sensitivity Differential Scanning Calorimetry
2D ^{1}H NMR NOESY	Two-Dimensional Proton NMR Nuclear Overhauser Effect Spectroscopy
DLS	Dynamic Light Scattering
SLS	Static Light Scattering
SAXS	Small Angle X-ray Scattering
SANS	Small Angle Neutron Scattering
REPES	Regularized Positive Exponential Sum
PDDF	Pair Distance Distribution Function
IFT	Inverse Fourier Transformation
DSC	Differential Scanning Calorimetry
MR	Molar Ratio
SI	Supporting Information
PD	Polydispersity
PAMPTMA	Poly((3-acrylamidopropyl) trimethylammonium chloride)
PAMPS	Poly(sodium 2-acrylamido-2-methyl-1-propanesulfonate)

1

Introduction

Amphiphilic molecules or amphiphiles play a vital role in our everyday life. Their task in the living systems as proteins, lipid membranes, bile salts, etc., their consumption in industry as surfactants, emulsifiers, stabilizers, etc., and their biomedical applications in controlled drug delivery, all reveal a touch of their important role. This vast field of applications is due to a novel structure of these molecules. Amphiphiles contain both polar and nonpolar domains. Depending on the solvent (polar or nonpolar) they are in contact with, amphiphiles are able to self-assemble and form aggregates such as micelles. In aqueous solutions, the nonpolar or hydrophobic domains arrange themselves in the core of the micelle, and the polar or hydrophilic domains occupy the surface of the micelle (corona) to reduce unfavorable interactions between the hydrophobic domains and water molecules.

Systems containing interesting amphiphiles such as block copolymers and a bile salt were studied in this thesis. Some of the general aspects of these amphiphiles that are relevant to this study will be described later in the current chapter (**Chapter 1**). **Chapter 2** includes the theory of the main experimental techniques applied in this study, and a summary of the results is covered in **Chapter 3**. The latter chapter is divided into two parts; **Part I** and **Part II**. In **Part I**, the focus is on the effects of bile salt sodium glycodeoxycholate (NaGDC) on the self-association of triblock copolymers of poly(ethylene oxide) (PEO) and poly(propylene oxide) (PPO), denoted as PEO-PPO-PEO. The motivation of **Part I** was to investigate the possibility of using PEO-PPO-PEO block copolymers as bile salt sequestrants in the therapy of *bile acid diarrhea* and *hypercholesterolemia* diseases. In **Part II**, attention is given to the charged poly(*N*-isopropylacrylamide) (PNIPAAM) diblock copolymers and their mixtures in aqueous solution. Due to their specific attributes, these block copolymers are potential candidates to be used in pharmaceutical and industrial applications. The aim of **Part II** was to study the physio-chemical behavior of these diblock copolymers, their response to different stimuli, and their interaction

with oppositely charged diblock copolymers in aqueous solution. **Chapter 4** contains the conclusions and future remarks. The papers are found at the end of the thesis.

1.1. Block Copolymers

A group of polymers that are formed by a covalent bond between two or more blocks of different polymerized monomers is called block copolymers. Among different structures of block copolymers, diblock copolymers (A-B) and triblock copolymers (A-B-C or A-B-A) have been vastly studied.[1] Other complicated architectures of block copolymers, such as graft or dendrimer-like, have also been synthesized.[2] Block copolymers can be used in a variety of applications as stabilizers, viscosity modifiers, nanocarriers in drug delivery and gene therapy, etc. [1, 3-6]

The solution properties of block copolymers can be tuned based on the quality of the solvent and features of the covalently bonded blocks.[7] If there is a difference in the hydrophobicity levels of the blocks, they show amphiphilic characteristics in aqueous solutions, which are quite similar to low molecular weight surfactants. In fact, amphiphilic block copolymers are polymeric surfactants. Hence they self-assemble and form for instance micelles, in addition to other types of self-organized structures (Figure 1.1).[8]
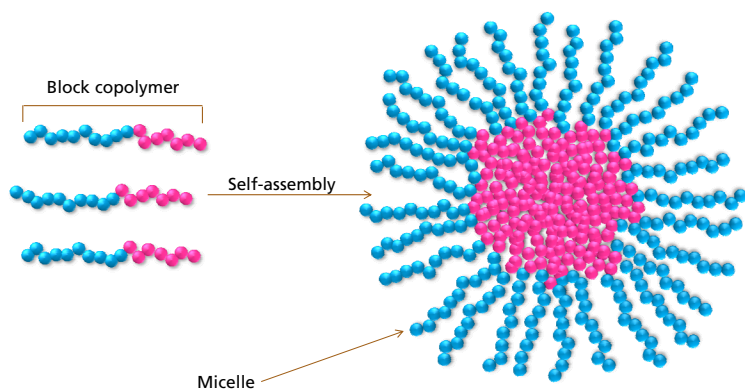
Figure 1.1. Schematic illustration of the amphiphilic block copolymer and its self-assembly in aqueous solution to form a micelle.

Depending on the chemical nature of the blocks, block copolymers can be classified as nonionic and ionic copolymers. The presence of charged blocks stabilizes the block copolymer micelles electrostatically. Mixed micelles composed of different block copolymers allow for an introduction of multi stimuli-responsive systems that are very attractive especially in drug delivery applications.[9] Thus block copolymers which are synthesized in a way that can

respond to different stimuli such as temperature, pH, ionic strength, etc., could be considered "smart materials".

The focus of this thesis is on one type of nonionic PEO-PPO-PEO triblock copolymers and one type of ionic diblock copolymers consisting of one block of PNIPAAM and a charged block. Details about the structure and some general features of these block copolymers relevant to the different studies are described in the following sections.

1.1.1. PEO-PPO-PEO Triblock Copolymers

Poly(ethylene oxide)-*b*-poly(propylene oxide)-*b*-poly(ethylene oxide) triblock copolymers, or briefly EO_n-PO_m-EO_n, (Figure 1.2), belong to the family of nonionic block copolymers.[10] Depending on the manufacturer, they are commercially named Pluronics, Poloxamers or Synperonics. Low toxicity and biocompatibility together with the fascinating physio-chemical characteristics qualify these polymers to be used in a lot of pharmaceutical applications.[6, 11]
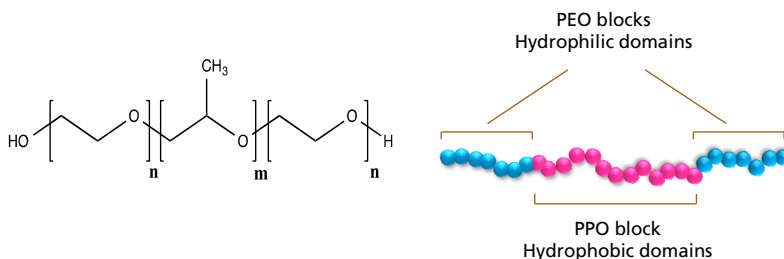
Figure 1.2. Chemical structure of EO_n-PO_m-EO_n block copolymer (left), and its schematic illustration with hydrophobic and hydrophilic domains (right).

They are considered to be amphiphiles and, due to the difference in the hydrophobicity of PEO and PPO blocks, they can act as polymeric surfactants. They self-assemble into micelles above a critical micelle temperature, CMT, and a critical micelle concentration, CMC. Because of the conformational change in EO and PO segments,[12-14] the hydrophobicity of both blocks increases upon an increase in temperature. However, this effect is more significant for PPO. Consequently the PPO block of the block copolymer is dehydrated via an endothermic process in which an increase in the entropy of the system due to the release of bound water molecules favors micellization.[15, 16]

Commercially, Pluronics can be produced with a wide range of different PPO and PEO block lengths. These polymers are usually polydisperse owing to the presence of mass and composition contaminants. Because of polydispersity, in addition to the gradual change in hydrophobicity of PPO with temperature, the block copolymers do not have a sharp CMC or CMT and may influence the structure of the liquid crystalline phases.[17-19] Studies show that the block

copolymers with a constant PPO/PEO ratio but with a higher molecular weight have lower CMT and CMC values. This behavior is also seen for block copolymers with a larger PPO block.[15]

In dilute solution, the PEO-PPO-PEO micelles usually have a spherical core-shell structure with a core consisting of mostly PPO and a shell including water and PEO.[14, 20-22] At elevated temperatures, water also becomes a poor solvent for PEO, hence micelles of some copolymers grow and change into rod-like structures (a sphere-to-rod transition).[23-25]

There are investigations which indicate that addition of ionic surfactants, such as sodium dodecyl sulfate, SDS, and cetyltrimethyl amonium chloride, CTAC, influences the self-assembly of the PEO-PPO-PEO block copolymers. Small surfactant-rich complexes are formed below CMC and CMT of the copolymer as a result of the cooperative association of the surfactant molecules on the PPO domains of the single block copolymer chains, i.e. unimers. This may enhance or suppress the block copolymer self-assembly. On the other hand, above CMC and CMT of the copolymer, polymer-rich complexes are formed due to the noncooperative association of surfactant molecules to block copolymer micelles. These complexes disintegrate at higher surfactant concentrations.[26-32]

In **Part I** of the thesis, effects of NaGDC on the self-assembly of three PEO-PPO-PEO block copolymers, P123, F127, and P65, were investigated and compared (**Paper I, II and III**).

1.1.2. PNIPAAM-Based Charged Diblock Copolymers

PNIPAAM (Figure 1.3) is known as a thermoresponsive amphiphilic polymer, which has a lower critical solution temperature, LCST about 32 ^{o}C in aqueous solution.[33] Despite the fact that PNIPAAM is rather hydrophobic, it is soluble in water below LCST as a result of favorable interactions via hydrogen bonds between its amide groups and water molecules. However, above LCST, water becomes a poor solvent for PNIPAAM due to the disruption of these hydrogen bonds in addition to the formation of intramolecular hydrogen bonds. In this state, water-water and PNIPAAM-PNIPAAM interactions become favorable rather than water-PNIPAAM interactions, and as a consequence the polymer undergoes a coil-to-globule transition.[34] This transition in dilute solution is associated with dehydration of the polymer chains, which is followed by a phase separation at temperatures above its clouding temperature or CP. It has been demonstrated that the CP of low molecular weight PNIPAAM polymers is suppressed by an increase in concentration and chain length of PNIPAAM.[35]
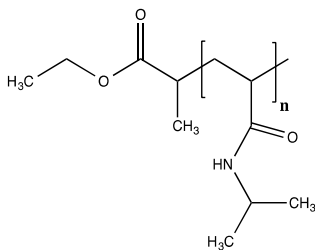
Figure 1.3. Chemical structure of poly(*N*-isopropylacrylamide), PNIPAAM.

Since the LCST for PNIPAAM is close to body temperature, it is considered one of the most interesting polymers to be used in drug delivery applications.[36] However, in order to be qualified for these types of applications, PNIPAAM unimers should be able to self-assemble and form micelle-like structures. Copolymerizing PNIPAAM with more hydrophilic or hydrophobic polymers, for instance by synthesizing block copolymers based on PNIPAAM, allows for the tuning of the novel characteristics to be optimal for the desired applications. As an example, attaching a hydrophilic polymer block improves the PNIPAAM water solubility above its LCST. At elevated temperatures and above CMC, these types of block copolymers can self-assemble as core-shell micelles, where the PNIPAAM segments form the core and the hydrophilic blocks the corona, to minimize the interfacial tension between water molecules and the PNIPAAM block. Attaching a charged block to PNIPAAM can generally improve its solubility and also the stability of the micelles, thanks to the electrostatic interactions that occur between them. Thus, depending on the characteristics of the attached block, PNIPAAM block copolymers can be responsive to other stimuli besides temperature, such as ionic strength and pH.

In **Part II** of this thesis, cationic diblock copolymers consisting of a charged block and a neutral PNIPAAM block of various lengths were characterized. The effects of PNIPAAM block length, temperature, polymer concentration, and salt addition on the association behavior of these block copolymers were investigated (**Paper IV**). Furthermore the characteristics of mixed solutions of the same kind of cationic block copolymers as above and a diblock copolymer composed of an anionic block and a PNIPAAM block of the same length as the cationic one were investigated (**Paper V**).

1.2. Bile Salts

Bile salts are amphiphilic molecules and are biological or natural surfactants.[37] Stored in the gallbladder, they are the end-product of the cholesterol metabolism in the liver. They help with fat digestion and uptake of fat-soluble vitamins in the intestine.[38]

There are two types of bile acids (unionized form of bile salts): primary (cholic and chenodeoxycholic acids) and secondary (deoxycholic and lithocholic acids). The secondary bile acids are produced in the intestine by microbial dihydroxylation of the primary bile acids. In humans, bile acids are mostly in a form of conjugated bile acid with glycine or taurine.[39] The bile salt that has been studied in this thesis (**Part I**) is NaGDC which is a secondary bile acid conjugated with glycine (Figure 1.4).
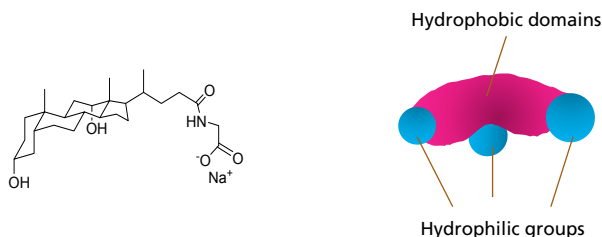
Figure 1.4. Chemical structure of sodium glycodeoxycholate, NaGDC (left) and a schematic illustration of a bile salt with hydrophobic domains and hydrophilic groups (right).

Bile salts are ionic surfactants, but some of their self-assembly characteristics are different from conventional ionic surfactants.[40] A flat and rigid steroid-like structure forms the hydrophobic domain while hydroxyl, acidic and amide (in the case of conjugated bile salt) are affected by their special structure and unusual distribution of hydrophobic and hydrophilic domains. It has been shown in simulations[41] and also with the help of some techniques[42] that micellization occurs in two steps, a primary and a secondary one. The primary step is attributed to the formation of small micelles, and the secondary step is related to stable micelle formations. Consequently, they do not have specific CMC values as classical ionic surfactants. Their CMC is rather identified as an interval of concentrations. Depending on the bile salt, the pH, and the ionic strength of the solution, they can form micelles or aggregates with globular, rod-like, or tubular shapes.[43-46] The solubility of the bile acids is pH dependent. The conjugated bile acids have a $pK_a < 3.9$,[47] which makes them soluble in the small intestine with a pH value of 5.5–7.

Bile salts undergo enterohepatic circulation via reabsorption (about 95% in a healthy adult) at the end part of the intestine and going back to the liver. The malabsorption causes the bile salts to enter the colon and stimulate secretion of water and electrolytes. This in turn is the reason for a disease called *bile acid diarrhea*.[48] In order to prevent diarrhea, patients are prescribed bile acid sequestrants which are cationic polymers. These sequestrants, such as cholestyramine for instance, act as ion exchange resins and interact with the bile salts both electrostatically and hydrophobically.[39] Although these sequestrants are very efficient, they have side effects such as constipation, bloating, nausea etc.,

which are unpleasant for the patients. Conversely, a high production amount of bile salts is favorable in the treatment of *hypercholesterolemia* disease. So in order to investigate the possibility of using block copolymers as bile acid carriers in the treatment of these two diseases, the effects of NaGDC on the self-assembly of three PEO-PPO-PEO block copolymers have been investigated in **Part I** of this thesis (**Paper I, II, and III**).

2
Main Techniques of Investigation

Different experimental methods of investigation were employed in the studies of this thesis, for instance various scattering techniques, high sensitivity differential scanning calorimetry (HSDSC), turbidimetry, electrophoretic mobility measurements, and two-dimensional proton NMR nuclear Overhauser effect spectroscopy (2D ^{1}H NMR NOESY). However this chapter only covers the theory of the most important ones, such as HSDSC and the scattering techniques that include dynamic and static light scattering (DLS and SLS), as well as small angle X-ray and neutron scattering (SAXS and SANS).

2.1. Scattering Techniques

Scattering techniques have been vastly used to study polymer, surfactant or polymer-surfactant mixed systems since many years. These techniques can provide useful information about the structure of particles, i.e. shape and size, as well as interparticle interactions. Moreover information about the dynamics of the particles in these systems could be obtained by the use of these techniques. It is worth mentioning that the extent of extracting such information depends on the type of scattering technique employed and also the properties of the studied system.

All scattering techniques are based on the same principle. The incident beam of radiation (a visible light, an X-ray or a neutron source) is passed through the sample and interacts with it. In general, part of the beam is transmitted, part of it is absorbed, and the rest of it is scattered by the sample.[49] In a scattering experiment, the focus is on the part related to the scattered radiation. The radiation wavelength (or the techniques) should be selected so that the samples have the smallest absorption possible when interacting with the radiation beam. In this thesis, elastic scattering techniques have been used in the different studies presented. In these types of methods, it is assumed that the frequency of the incident and the scattered radiation are the same, and hence there is no energy loss.[49]

The scattering intensity is detected by a detector at a chosen scattering angle θ, which is the angle between the wave vector of the incident beam $\vec{k}_i$ and that of the scattered beam $\vec{k}_s$. The scattering vector $\vec{q}$ is obtained by the subtraction of $\vec{k}_s$ from $\vec{k}_i$ (Figure 2.1), and its absolute value is calculated as follows:

$$q = \frac{4\pi \sin\left(\frac{\theta}{2}\right)}{\lambda} \qquad (1)$$

where λ is the wavelength of the incident beam.
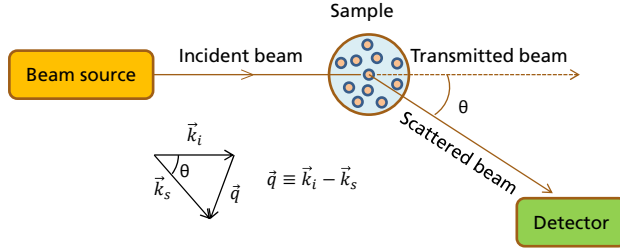
Figure 2.1. A schematic illustration of a scattering experiment and definition of the scattering vector, $\vec{q}$.

To be able to identify the suspended particles in the medium with the scattering techniques, there should be a contrast variation between for example the solvent molecules and the suspended particles. This contrast originates from the difference in density of the scattering particles in the medium.[50] Depending on the type of radiation source and its interaction with the medium, the contrast term differs from one scattering technique to another. Further explanation of the contrast term in the scattering techniques will be given briefly in the following sections.

2.1.1. Light Scattering

The radiation source in the light scattering technique is a laser beam. It is a source of monochromatic plane-polarized light with a wavelength in the visible part of the spectrum (in this study $\lambda = 632.8 \, nm$). Just as other types of radiation, light is an electromagnetic wave. The electric field of this wave at position $\vec{r}$ is defined as:[50]

$$E_i(\vec{r}, t) = E_0 exp\left[i\left(\vec{k}_i \cdot \vec{r} - \omega t\right)\right] \qquad (2)$$

where E_0 is the amplitude of the electric field, and $\vec{k}_i$ is the wave vector of the incident field which has a magnitude of $2\pi n/\lambda$ (in case of light scattering), where n is the refractive index of the medium and ω is the angular frequency. When the polarized beam of light is passed through the sample, it interacts with the electrons of the atoms in the medium and induces oscillating dipoles. These

dipoles are oscillating polarizations of electrons in the medium and they act as a supply for the scattered light.[50, 51] The dipole momentum of the scattered light, $\vec{m}$, is related to the polarizability of the atom, α, and the electric field of the incident light, $\vec{E}_i$:

$$\vec{m} = \alpha \vec{E}_i \tag{3}$$

For N scattering particles in the scattering volume V, polarizability is related to the dielectric permittivity ε and the refractive index n, as follows:[52]

$$4\pi \frac{N}{V} \alpha = \varepsilon - 1 = n^2 - 1 \tag{4}$$

The amplitude of the scattered electric field, E_S from N particles in the scattering volume V is defined as:[50]

$$E_S(\vec{R}, t) = -E_0 \frac{exp[i(kR - \omega t)]}{R} \sum_{j=1}^{N} b_j(\vec{q}, t) \, exp[-i\vec{q}.\vec{R}_j(t)] \tag{5}$$

where $k = |\vec{k}_s|$, $\vec{R}$ is the distance vector between the detector and the sample with magnitude R, and $b_j(\vec{q}, t)$ is the scattering length of particle j defined as:[50]

$$b_j(\vec{q}, t) = \int_{V_j} \Delta\rho(\vec{r}_j, t) exp(-i\vec{q}.\vec{r}_j) \, d^3 r_j \tag{6}$$

where $\Delta\rho$ is the excess scattering length density, which is the contrast term in the light scattering method.

The excess scattering length density is related to the refractive index of the material by equation (7), which is calculated as follows:[50]

$$\Delta\rho(\vec{r}_j, t) = \frac{k^2}{4\pi} \left[\frac{n^2(\vec{r}_j, t) - n_L^2}{n_0^2} \right] \tag{7}$$

$n(\vec{r}_j, t)$ is the refractive index of the scattering particles at position $\vec{r}_j$, n_L is the average refractive index of the liquid, and n_0 is the average refractive index of the whole sample.

The scattering intensity, I_S is defined as:

$$I_S(\vec{q}, t) = |E_S(\vec{q}, t)|^2 \tag{8}$$

and using equation (5), it is described as:

$$I_S(\vec{q}, t) = \left(\frac{E_0}{R} \right)^2 \sum_{j=1}^{N} \sum_{k=1}^{N} b_j(\vec{q}, t) \, b_k(\vec{q}, t) \, exp\left[-i\vec{q}. \left(\vec{R}_j(t) - \vec{R}_k(t) \right) \right] \tag{9}$$

Static Light Scattering

In order to get information about the size, shape, and interparticle interactions of the suspended particles in an isotropic solution, the time-averaged intensity of the scattering light is required:[50]

$$\langle I_S(q) \rangle = \left(\frac{E_0}{R}\right)^2 \left\langle \sum_{j=1}^{N} \sum_{k=1}^{N} b_j(\vec{q}) \, b_k(\vec{q}) \, exp\left[-i\vec{q}.\left(\vec{R}_j - \vec{R}_k\right)\right]\right\rangle \tag{10}$$

Thus, by measuring the time-averaged scattering intensity in a static light scattering experiment, the excess Rayleigh ratio, ΔR_θ, can be obtained:

$$\Delta R_\theta = \frac{I_S(\theta) - I_0(\theta)}{I_{ref}(\theta)} R_{ref}(\theta)(\frac{n}{n_{ref}})^2 \tag{11}$$

where $I_S(\theta)$, $I_0(\theta)$, and $I_{ref}(\theta)$ are the scattering intensities of the solution, the solvent, and the reference (usually toluene) at angle θ, respectively. $R_{ref}(\theta)$ is the Rayleigh ratio of the reference at angle θ, and the refractive indices of the solution and the reference are n and n_{ref}, respectively.

ΔR_θ is related to the molecular weight of the scattering particles as well as the interparticle interaction.[49] Since the calculation of the latter quantities was not covered in this study, further derivations are not needed.

Dynamic Light Scattering

Particles in the solution undergo Brownian motion and their local concentration fluctuates in time. Hence the intensity of the light scattered by the solution fluctuates in time as well. Studying how the fluctuations change over time is done in a DLS experiment. It may give information about the translational diffusion of the particles, from which a calculation of the particle size is possible.

In a dynamic light scattering experiment, the normalized time correlation function of the scattered intensity $g^{(2)}(q,t)$ is reported. It is defined as:[53]

$$g^{(2)}(q,t) \equiv \frac{\langle I(q,0)I(q,t)\rangle}{\langle I(q)\rangle^2} \tag{12}$$

where $I(q,0)$ and $I(q,t)$ are the scattered intensity at time 0 and a delayed time t, respectively.

The normalized time correlation function of the scattered electric field $g^{(1)}(q,t)$ is related to $g^{(2)}(q,t)$ by the Siegert relation as:[54]

$$g^{(2)}(q,t) = 1 + \beta\left[g^{(1)}(q,t)\right]^2 \tag{13}$$

where $\beta \leq 1$ is an instrumental parameter which accounts for the deviation from ideal correlation and depends on experimental geometry.

22

In the case of a system containing monodisperse spherical particles, $g^{(1)}(q,t)$ can be fitted to a single-exponential function with a characteristic relaxation time, τ. In the case of a polydisperse system containing a range of particle sizes, $g^{(1)}(q,t)$ can be expressed in terms of a Laplace transformation of a distribution of relaxation times, $A(\tau)$:

$$g^{(1)}(q,t) = \int_{-\infty}^{+\infty} \tau A(\tau) exp(-t/\tau) dln\tau \tag{14}$$

All DLS data in this thesis except in **Paper IV** have been analyzed for retrieving $A(\tau)$ with the help of a constrained nonlinear regularization algorithm called Regularized Positive Exponential Sum (REPES).[55] REPES analyzes the measured $g^{(2)}(q,t)$ data based on the model given in equation (14).

In the case of **Paper IV**, DLS data have been analyzed with a nonlinear fitting algorithm to obtain the best-fit values. In this data analysis, the field correlation function was fitted to either a biexponential or a single exponential function:

$$g^{(1)}(q,t) = A_f exp(-t/\tau_f) + A_s exp\left[-(t/\tau_s)^{\beta}\right] \tag{15}$$

$$g^{(1)}(q,t) = exp\left[-(t/\tau_s)^{\beta}\right] \tag{16}$$

where A_f and A_s are the amplitudes of the fast and the slow modes of motion, respectively ($A_f + A_s = 1$), τ_f and τ_s are the relaxation times of the fast and the slow mode, respectively, and β is the stretched exponent related to the width of the relaxation time distribution.

The collective translational diffusion coefficient, D is defined as:

$$D = \lim_{q \to 0}(\Gamma/q^2) \tag{17}$$

where $\Gamma (= 1/\tau)$ is the relaxation rate.

D_0 is the diffusion coefficient at the infinite dilute concentration. It can be calculated by studying the concentration dependence of D and can be applied to calculate the hydrodynamic radius of the particles, R_H, by using the Stock-Einstein equation:

$$R_H = \frac{kT}{6\pi \eta_0 D_0} \tag{18}$$

where k is the Boltzmann constant and η_0 is the viscosity of the solvent at the absolute temperature T. However, using D instead of D_0 in equation (18) provides the apparent hydrodynamic radius $R_{H,app}$, which is influenced by both hydrodynamic and interparticle interactions.

2.1.2. Small Angle X-ray and Neutron Scattering

In the SAXS and SANS techniques, the radiation source is the X-ray and neutrons, respectively. Generally, small angle scattering techniques help in exploring the smaller length scales in the material compared to light scattering techniques. In both techniques, the electric field of the scattered radiation from the sample is defined by equation (5). However, the only difference is the way that the contrast term $\Delta\rho$ is expressed. This in turn influences the calculation of $b_j(\vec{q}, t)$. The X-ray beam interacts with the electrons of the material. Thus, in a SAXS experiment, the excess scattering length density is defined as:[52]

$$\Delta\rho(\vec{r}_j, t) = \frac{r_e}{V}\left(\sum_j Z_j - \sum_k Z_{k,L}\right) \tag{19}$$

where V is the volume of the particle, $r_e = 2.81794 \times 10^{-5}$Å is the electron radius, and Z_j and $Z_{k,L}$ are the numbers of electrons in the molecule or atom of the particle and the solvent, respectively. It can be noted from equation (19) that the higher the number of electrons in the atoms, the higher scattering intensity.

In a SANS experiment, the neutron beam interacts with the atom nucleus instead, so $\Delta\rho$ is then expressed as:

$$\Delta\rho(\vec{r}_j, t) = \frac{1}{V}\left(\sum_j b_j - \sum_k b_{k,L}\right) \tag{20}$$

where b_j and $b_{k,L}$ are the coherent scattering lengths of the molecules or the atoms of the particle and the solvent, respectively.

Although equations (5)–(10) are also valid in the case of SANS and SAXS experiments, a more common way of expressing the intensity of the scattered beam is:

$$I(q) = \phi V P(q) S(q) \tag{21}$$

where ϕ is the volume fraction of the particles, $P(q)$ is the form factor and it is related to the intraparticle interference, i.e. the size and shape of the particle, and $S(q)$ is the structure factor which is connected to the interparticle interactions.

The scattering intensity is usually analyzed in two ways, a model-free or a model-dependent analysis. In the model-free analysis, no prior information is needed to fit the data. This type of fitting is based on the inverse Fourier transformation of the scattering intensity which results in retrieval of the pair distance distribution function PDDF or $p(r)$. In the model-dependent analysis, the scattering intensity is fitted using the $P(q)$ and $S(q)$ given by analytical models which have been defined already, or given by a model that is written

based on the characteristics of the system being studied.[56] In the different studies of this thesis, both types of analysis have been employed. The equations and the description regarding the analysis can be found in the supporting information, **SI** of **Paper I, II, III and V.**

2.2. High Sensitivity Differential Scanning Calorimetry

Differential scanning calorimetry is an appropriate technique for studying the thermal (exothermic or endothermic) events (transitions) such as phase transitions or conformational changes in polymer and surfactant systems. For instance, to study the micelle formation of block copolymers that show a heat-induced micellization in solutions, DSC could be a helpful technique for determining the enthalpy of micellization and the critical micelle temperature.

The DSC instrument has two identical cells which are filled with identical volumes of the sample and the reference solution, respectively. It is equipped with a sensitive temperature sensor and heaters. In a DSC measurement the difference in the heat capacity C_P of the sample and the reference cell is reported against the temperature. A thermal transition is determined by a peak which is related to the apparent molar heat capacity of the sample, C_P^{app}. The area under the peak is considered to be the enthalpy of transition, ΔH_{tr} (Figure 2.2):[57]

$$\Delta H_{tr} = \int_{T_{onset}}^{T_{end}} C_P^{app} \, dT \tag{22}$$

T_{onset} and T_{end} are the temperatures at which the transition begins and ends, respectively. The temperature corresponding to the peak maximum is denoted T_m. In case of a heat-induced micellization process, T_{onset} may be considered as CMT. The narrower peak demonstrates the presence of high cooperativity between the molecules in the transition event. The results from this technique for the present study can be found in **Paper I, III, and VI.**
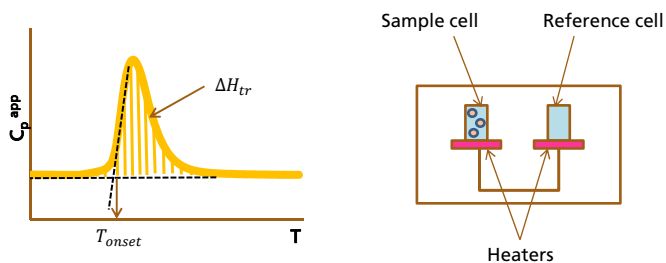

Figure 2.2. A thermogram of a transition with the onset temperature, T_{onset} and the enthalpy of transition, ΔH_{tr} obtaind from a DSC experiment (left) and a schematic illustration of a DSC instrument (right).

3

Summary of Results

Part I

3.1. Effects of Bile Salt NaGDC on the Self-Association of PEO-PPO-PEO Block Copolymers

The overall purpose of **Part I** of the thesis was to investigate the possibility of using PEO-PPO-PEO block copolymers as bile acid sequestrants in the therapy of *bile acid diarrhea* and also in the treatment of *hypercholesterolemia* diseases. Achieving these aims primarily requires exploration of a less complex system. Thus, it was necessary to study the basic physio-chemical behavior of the individual polymers in dilute aqueous solution as well as their aqueous mixtures with bile salt. The investigation was initially started by studying a mixed system of one type of selected block copolymers, $EO_{20}PO_{68}EO_{20}$ denoted P123, and one bile salt, NaGDC. This study was helpful in determining whether there is a similarity in the behavior of a bile salt and other classical ionic surfactants in interaction with these types of block copolymers. The next step was to find out how the relative length of the PEO and PPO segments influences the interactions in the mixtures of PEO-PPO-PEO polymers and NaGDC. Hence two other block copolymers, F127 ($EO_{97}PO_{69}EO_{97}$) and P65 ($EO_{19}PO_{29}EO_{19}$) with a longer PEO block and a shorter PPO block compared to P123 respectively, were investigated.

3.1.1. Pure P123 and NaGDC Solutions (Paper I)

A DSC measurement on an aqueous solution of 1.74 mM (1 wt %) P123 revealed that it is a thermoresponsive system. The thermogram had a main endothermic transition peak with the onset temperature at T_{onset} =17.6 ^{o}C. This transition peak is associated with dehydration of PPO blocks of the single polymer chains (unimers) during the micelle formation process. Hence the T_{onset} and the area under the peak are defined as the critical micelle temperature, CMT, and the

enthalpy of micelle formation, ΔH_{tr}, respectively (Table S1 in Supporting Information, SI and Figure 1, **Paper I**). The second endothermic peak is due to the sphere-to-rod transition of the P123 micelles that appear at higher temperatures with a peak maximum at $T_m = 61.9\ ^\circ$C (Figure 3.1).
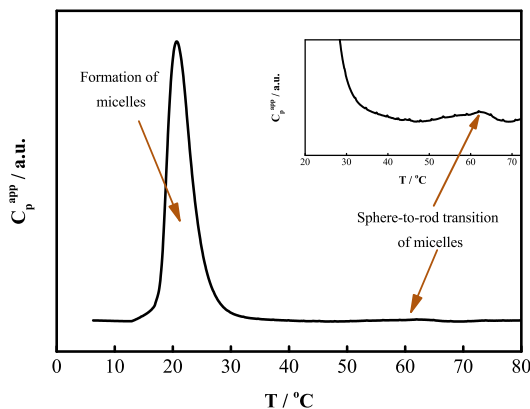
Figure 3.1. DSC curve of a 1.74 mM P123 aqueous solution. The inset is a magnification of a region where the sphere-to-rod transition of micelles occurs.

DLS measurements on the same solution were in line with the DSC results. The corresponding relaxation time distributions ($A(\tau)$) (Figure 3a in **Paper I**), varied from a bimodal distribution of P123 unimers and clusters (contaminants with polydispersity in mass and composition) at 15 $^\circ$C, to a monomodal distribution of P123 micelles at 40 $^\circ$C ($R_{H,app}$ =9.8 nm), where the micellization of P123 unimers was complete based on the DSC results. Finally at 60 $^\circ$C, although the relaxation time distribution was monomodal, it shifted to slower times due to the growth of P123 micelles in the vicinity of the sphere-to-rod transition.

To the contrary, no transition peak was observed in the DSC thermogram of a pure NaGDC solution with a concentration of 95.8 mM (Figure 3.2). This observation was completely mirrored in the DLS results (Figure 3b in **Paper I**), where the relaxation time distributions displayed a similar monomodal behavior at all studied temperatures (20–60 $^\circ$C). According to the literature NaGDC has a CMC of 3–6 mM,[42] hence the distribution corresponded to the negatively charged NaGDC micelles.

3.1.2. Mixed P123-NaGDC Solutions (Paper I and II)

In order to investigate the effects of NaGDC on the self-assembly in water of the P123 block copolymers, the concentration of P123 was kept constant at 1.74 mM, i.e. 1 wt %, while the concentration of NaGDC was varied up to 250 mM. In comparison with the pure P123 solution, the DSC results demonstrated that

adding NaGDC does not significantly influence the main transition peak. T_{onset} was constant up to a molar ratio MR=0.6 (MR= n_{NaGDC}/n_{P123}), but a small decrease in ΔH_{tr} was observed (Table S1 in SI, **Paper I**). At MR>5.6 where the concentration of NaGDC was well above the CMC, the effects of the NaGDC addition were clearly observed (Table S1 in SI, **Paper I** and Figure 3.2):

a) T_{onset} increased, i.e., the CMT of P123 increased.

b) Transition peaks became wider, meaning that the cooperativity of the micelle formation of P123 was suppressed.

c) ΔH_{tr} decreased which indicated that the number of PPO units contributing in the micellization process decreased.

d) At MR>12, and at temperatures below the T_{onset} of the main transition peak, a broad endothermic peak was detected. This revealed that the PPO units were dehydrated in another type of mechanism (Figure S1 in SI, **Paper I**).
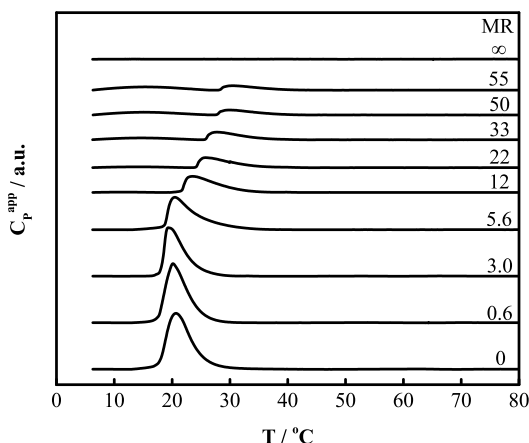
Figure 3.2. DSC curves of a 1.74 mM P123 aqueous solution with various amount of NaGDC (MR= n_{NaGDC}/n_{P123}). MR=∞ is related to a 95.8 mM NaGDC solution.

At 40 ^{o}C, which is well above the CMT of the pure P123 solution (MR=0) (Figure 3.1), the DLS measurements on the mixed P123-NaGDC solutions clearly pointed to the presence of three concentration regimes, which were in good agreement with the SLS results (Figure 5b in **Paper I**). The following observations describe the characteristics of these regimes as the NaGDC concentration increased in the system:

a) One *low* concentration regime (MR≤0.6) with a monomodal behavior of the relaxation time distributions, which was connected to the translational diffusion of the P123 micelle-NaGDC complexes (Figure 4a in **Paper I**) and a sharp increase in the reduced apparent diffusion coefficient ($D \eta_0/T$) (Figure 3.3). In

this regime the concentration of NaGDC was below the CMC of NaGDC. The reason for the increase in $D\eta_0/T$ was evidently associated with the formation of P123 micelles-NaGDC complexes in which NaGDC monomers interacted with the P123 micelles. These complexes were negatively charged due to the presence of GDC$^-$ ions and became increasingly so. This caused an increase in the repulsive electrostatic interaction between the complexes which accelerated the diffusive motion. This interpretation was confirmed by the observation of a decrease in the electrophoretic mobility of the complexes (Figure 6 in **Paper I**) and a suppression of the increase in $D\eta_0/T$ upon addition of salt to the solution (100 mM NaCl) (Figure 3.3). The latter was attributed to the screening of these electrostatic interactions. The SAXS results validated this interpretation even further by demonstrating a decline in the $S(q)$ in the low q region. However the IFT analysis of the SAXS data showed that there was a minor decrease in the size of complexes, which may slightly influence the translational diffusion, but it was negligible compared to the effect of the charge (Figure 7 in **Paper I** and Figure 2 in **Paper II**).
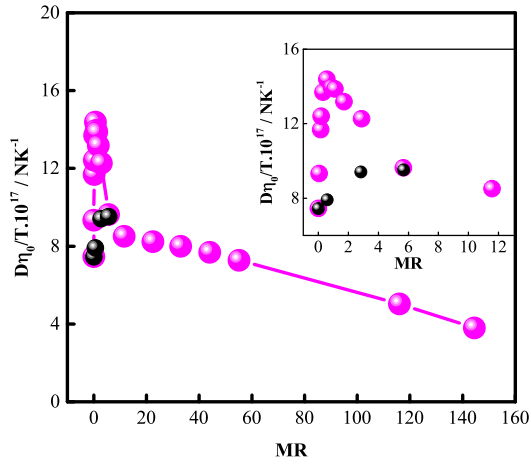
Figure 3.3. Reduced diffusion coefficient ($D\eta_0/T$) of a 1.74 mM P123 aqueous solution with various amount of NaGDC at 40 ^{o}C as a function of MR obtained from DLS data (pink symbols). The inset demonstrates the data in the low and intermediate concentration regimes. Also shown are the DLS data for solutions with 100 mM NaCl (black symbols).

b) One *intermediate* concentration regime (0.6≤MR≤12) with a monomodal behavior of the relaxation time distributions and a steep decrease in $D\eta_0/T$ (Figure 3.3). This regime was a crossover between the low and the high concentration regimes. Towards the higher NaGDC concentrations in this regime, the P123 micelle-NaGDC complexes could not accommodate more NaGDC monomers because of the repulsion between the associated GDC$^-$ ions in the complexes. Thus, the excess bile salt in the form of GDC$^-$ and Na$^+$ ions

30

and/or NaGDC micelles at higher bile salt concentrations screened the repulsive interaction between the P123 micelle-NaGDC complexes (Figure 6 in **Paper I**).

c) One *high* concentration regime (MR≥12) with a bimodal relaxation time distribution. The fast mode had a mean relaxation time identical to that of pure NaGDC, and its amplitude increased with increasing bile salt content in the solutions (Figure 4b in **Paper I** and Figure 3.4**)**. The slow mode became wider and shifted to longer decay times with increasing MR. Consequently, a steady decrease in $D\eta_0/T$ of the slow mode was monitored (Figure 3.3). In the light of the DSC and DLS results together with the knowledge that the concentration of NaGDC was well above its CMC in this regime, it was proposed that two complexes coexisted in this regime; the P123 micelle-NaGDC complexes, which started to disintegrate at higher MR and rearranged into polydisperse clusters of unidentified structure, and small NaGDC-P123 (or NaGDC-rich) complexes, which were NaGDC micelles interacting with one or several P123 unimers. The presence of the latter complexes was very well verified with a stoichiometric model (SI, **Paper I**) which was based on the experimental DSC results where the changes in the fraction of P123 unimers in these complexes as a function of NaGDC concentration was demonstrated (Figure S2 in SI and Figure 2, **Paper I**).
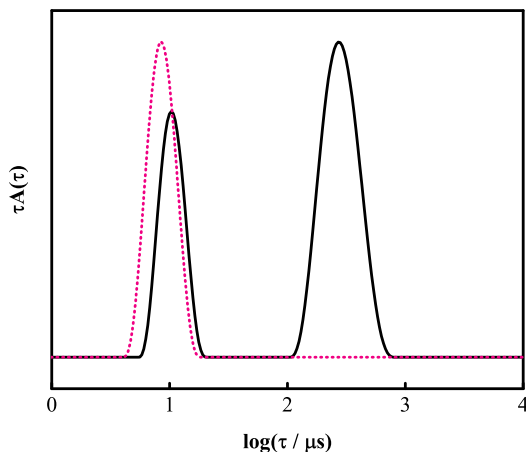
Figure 3.4. Relaxation time distributions for a 1.74 mM P123 solution at MR=144 (black line) and for a 95.8 mM NaGDC aqueous solution (red dotted line) at 40 ºC.

3.1.3. Complex Structure and Interactions in the P123-NaGDC System (Paper II)

To be able to use P123 micelles as carriers for bile salt monomers, the first and most essential consideration is that the NaGDC/P123 molar ratio should be kept at a level where the bile salt molecules cannot disintegrate the P123 micelles. It is also important to explore the internal structure of the complexes as well as the intercomplex interactions. Therefore SANS and SAXS techniques were

employed to study the P123 micelle-NaGDC complexes at 40 °C. The experiments were performed on solutions with molar ratios in the range MR=0–5.7 at a constant P123 concentration of C_{P123} =1.74 mM.

The pair distance distribution function ($p(r)$) obtained from the inverse Fourier transformation (IFT) analysis of the SAXS data revealed an inhomogeneous core-shell structure of the P123 micelle-NaGDC complexes at all molar ratios investigated. However, the observed decrease in the maximum radius ($D_{max}/2$ where D_{max} is the maximum dimension of the complexes) by addition of NaGDC from 10.1 to 8.3 nm (for MR=0 to MR=5.7) suggested a possible change in the inner structure of the complexes (Figure 2a in **Paper II** and Figure 3.5).
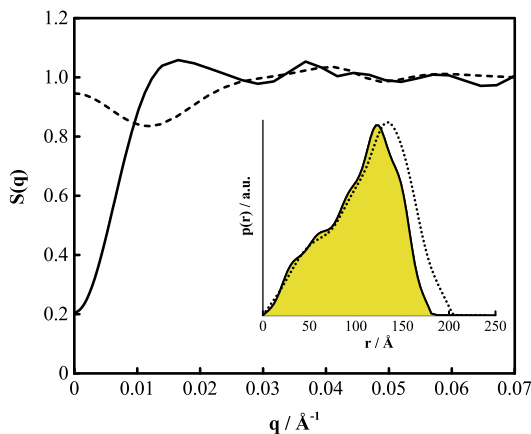
Figure 3.5. Structure factor curves from IFT analysis of SAXS data for a 1.74 mM P123 aqueous solution with various amount of NaGDC at 40 °C, MR=0.6 (solid line) and MR=5.7 (dashed line). The inset shows the $p(r)$ functions obtained from IFT analysis of the SAXS data for MR=0 (dotted line) and MR=0.6 (solid line with a yellow area).

The spherical core-shell and the Hayter-Penfold analytical models of form and structure factors, respectively, were applied to fit the SAXS and SANS curves (except for MR=0 where no structure factor was needed). The fact that the contrasts of the materials (Table 1 in **Paper II**) were different in a combination of these two techniques was very valuable for the interpretation of the results. Accordingly, it demonstrated the importance of using SAXS and SANS as complementary techniques in this study. In the fittings, it was assumed that the core mostly consisted of PPO and water and the shell mostly of PEO and water. Therefore the NaGDC monomers due to their amphiphilicity could target the core and/or the shell. Moreover, based on the negligible difference in the ΔH_{tr} values obtained from the DSC experiments (Table S1 in SI, **Paper I**), it was assumed that there was no change in the aggregation number of P123 in the micelles up to MR= 0.6.

The fitting results strongly confirmed the IFT analysis and also provided more details about the inner structure of the complexes and the intercomplex interactions. Analyses showed that the NaGDC monomers initially located themselves closer to the core/corona interface, causing a decrease in core size by rearrangement of the PPO chains and expulsion of some water molecules from the core. In this stage, the shell swelled to accommodate NaGDC monomers and likely some water molecules (Table A.1, A.2 in SI and Figure 4, **Paper II** and Figure 3.6).
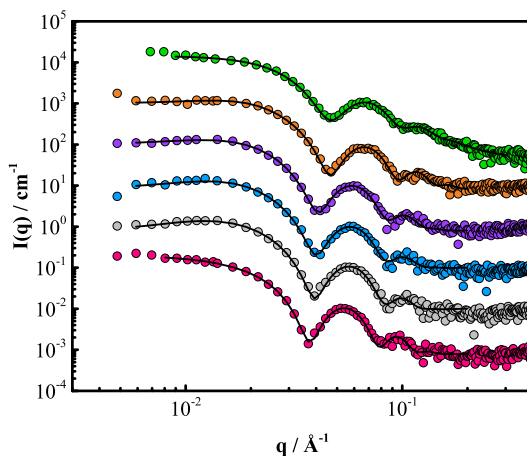
Figure 3.6. Scattering curves of a 1.74 mM P123 aqueous solution with various amount of NaGDC obtained from SAXS experiments at 40 $^{\circ}$C (symbols) together with the fitted curves (solid black lines). MR=0 (pink), MR=0.32 (grey), MR=0.59 (blue), MR=0.83 (violet), MR=3.1 (orange) and MR=5.7 (green).

These interpretations were compatible with the change in the scattering length densities of the core and the shell obtained from SAXS and SANS data analyses (Figure 5 in **Paper II**). The results from the SAXS measurements illustrated that at higher NaGDC concentrations (MR$\geq$0.8), the complexes, which were saturated with bile salt molecules, started to disintegrate and form small NaGDC-rich complexes. This interpretation was mirrored in the decrease of the shell thickness, although no significant change in the core radius was observed (Figure 4 in **Paper II**). The latter was due to the inclusion of some water molecules in the core, which was verified by scattering length densities obtained from SAXS data analysis (Figure 5 in **Paper II**). Also the enhancement of the polydispersity, PD by addition of NaGDC was a strong indication that disintegration of P123 micelle-NaGDC complexes occurred at higher MRs (Table A.1 and A.2 in SI, **Paper II)**. In contrast, the complexes in D_2O were more resistant to disintegration than those at the same MR in H_2O. This coordinates well with the study[58] that demonstrated that PEO-PPO-PEO block copolymers have a lower CMC and CMT in D_2O than in H_2O. Both the SAXS and SANS results showed

also that the total size of the complexes decreased by addition of NaGDC. In the case of SAXS at MR≤0.6 and SANS at all studied molar ratios, this decrease was due to the contraction of the core as a result of the bile salt association to the corona. However, the observed decrease in the total size of the complexes obtained from the SAXS data analysis was due to the disintegration of the complexes that started to occur at MR≥0.8.

The presence of GDC^- ions in the PEO corona of the complex was manifested in the structure factor analysis. The results from the IFT analysis of the SAXS data indicated that the repulsive intercomplex interaction increased (i.e., a lowering of the forward scattering, S(0)) up to MR≤0.6 whereafter it declined (i.e., higher S(0)) as the amount of NaGDC in the solutions increased (Figure 2b in **Paper II**). The interpretation of such behavior was elucidated by analysis using a structure factor of a system of charged hard spheres that interact via a repulsive screened Coulomb pair potential, calculated using the Hayter-Penfold method (see SI, **Paper III**).[59] This model, which is defined for systems containing a simple salt (1:1 electrolyte), showed that the negative charge of the complex was augmented by addition of NaGDC to the solution. Based on the assumption that not all NaGDC molecules were associated to the P123 micelles, the efficiency of intercomplex interaction was screened as the number of free GDC^- and Na^+ ions as well as possibly NaGDC micelles and NaGDC-P123 complexes increased. The latter two were not assumed to be simple salt in the fitting model. Hence the charge of the complexes was underestimated by the analysis in this study. Addition of sufficient amounts of salt to these solutions strongly confirmed the effect of repulsive intercomplex interactions on the translational diffusion of the P123 micelle-NaGDC complexes (Figure 6 in **Paper II**).

3.1.4. Pure P65 and F127 Solutions (Paper III)

In order to gain a better understanding of the effect of NaGDC on the self-assembly of P65 and F127 block copolymers, initially the self-assembly of pure block copolymers was investigated. Similar to the P123 block copolymer, the micelle formation of P65 and F127 was accompanied by a dehydration of PPO blocks. The dehydration process was manifested as an endothermic transition peak in the DSC thermograms (Figure S3b in SI and Figure 1 and 3b, **Paper III**) for all studied concentrations, 0.5–10 wt % (in the case of P65) and 1 and 5 wt % (in the case of F127). For both polymers, the CMT decreased upon increasing polymer concentration whereas ΔH_{tr} increased due to the availability of more block copolymer unimers in the micellization process (Table S1, S4 and S5 in SI, **Paper III**). The higher CMT values for the 1 wt % solutions of the P65 and F127 (38.1 ^{o}C and 25.3 ^{o}C, respectively) compared to that of a 1 wt % P123 solution (17.6 ^{o}C) (Table S1 in SI, **Paper I**) were associated with their lower hydrophobic-to-hydrophilic balance, i.e. number of PO units/number of EO units

(PPO/PEO ratio), (P123 (1.7) > P65 (0.76) > F127 (0.36)), together with the effects of the difference in molecular weight and PPO block length.

The DLS measurements on 1 wt % P65 solution (Figure S1b in SI, **Paper III**) as a function of temperature demonstrated that P65 unimers were in coexistence with clusters of hydrophobic contaminants at 20 °C. However, at 30 °C the presence of P65 micelles in the solution was clear according to the corresponding relaxation time distribution. At 50 °C only P65 micelles with a $R_{H,app}$ of 6.43 nm were present in the solution (Figure 3.7). These DLS results were in good agreement with the DSC and SLS data obtained for the same solution (Figure S2 and Table S1 in SI and Figure 1, **Paper III**).
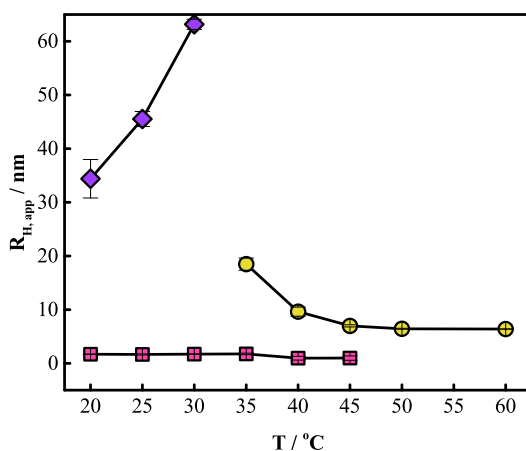
Figure 3.7. Temperature dependence of the apparent hydrodynamic radii $R_{H,app}$ of P65 unimers (pink symbols), micelles (yellow symbols) and clusters (violet symbols). The error bars are visible inside the symbol when smaller than the symbol size.

3.1.5. Mixed P65-NaGDC and F127-NaGDC Solutions (Paper I and III)

In order to study the effect of NaGDC on the self-assembly of P65 and F127, five block copolymer-NaGDC mixed solutions with fixed polymer concentrations of 1 or 5 wt % and with MR ranging from 0 to 12 were studied. The results demonstrated that small additions of NaGDC to the solutions induced micellization of both P65 and F127, i.e., a reduction in their CMT values was measured (Figure S3 and Table S2-S5 in SI, **Paper III** and Figure 3.8). A similar synergy effect was observed in the case of the F127-SDS system, where it was hypothesized that the interaction between the F127 unimer and the SDS micelle involves dehydration of the hydrated parts of the unimer.[27, 60] This could induce micelle formation of the block copolymer. The effect was more significant in the case of P65. The reason why the effect did not occur in the case of P123 is not clear but it may be related to the PPO/PEO composition ratio. On the other hand

the enthalpy of micellization for both polymers decreased more significantly by larger addition of the NaGDC. As previously mentioned (section 3.1.2), this decrease was related to the decreasing number of dehydrated PPO segments (Figure 3.8).
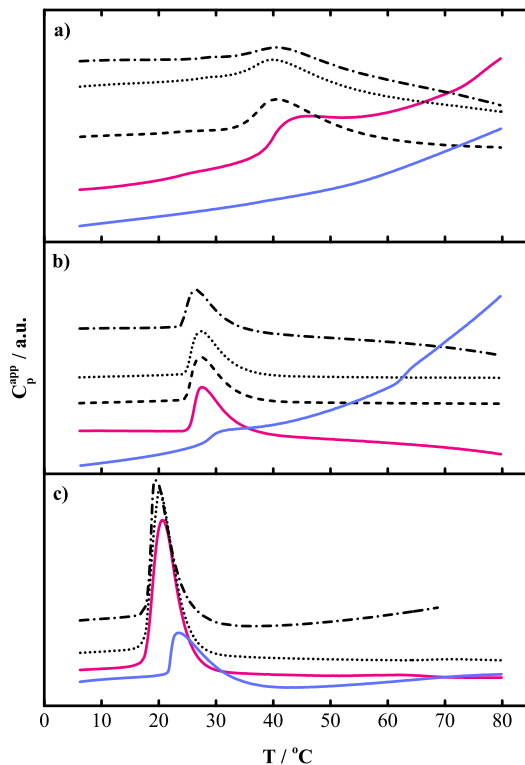
Figure 3.8. DSC curves for PEO-PPO-PEO block copolymer-NaGDC mixed solutions at various MR a) P65-NaGDC solutions, b) F127-NaGDC solutions and c) P123-NaGDC solutions. MR=0 (pink line), MR=0.3 (dashed line), MR=0.6 (dotted line), MR=3 (dashed dotted line) and MR=12 (blue line). The block copolymer concentration was 1.0 wt %.

DLS measurements were performed on the F127 and P65 systems at 50 ^{o}C where the relaxation time distributions were monomodal due to the diffusion of pure micelles/complexes. This mode shifted to faster times at higher molar ratios due to the formation of charged PEO-PPO-PEO micelle-NaGDC complexes. The effect of NaGDC on the self-assembly of P65 and F127 was very similar to that of P123 (Figure 3.9), however increasingly stronger in the case of P65 and unexpectedly weaker for F127. This behavior was completely different than what was expected based on the order of the PPO/PEO balance (see above). It was better related to the CMT which decreases in the order P123<F127<<P65. This order represents the tendency of the block copolymer to form micelles and it is reasonably connected with the micelle stability. The CMT is also affected by the

molecular weight and PPO block length. It is therefore expected that P123 micelles would have slightly higher resistance with the respect to the F127 micelles. However, this was not observed when comparing the relaxation time distributions. This may be related to the presence of the long PEO chains in the micellar corona that sterically hindered the association of NaGDC, and hence the F127 micelles were more resistant towards being disintegrated.
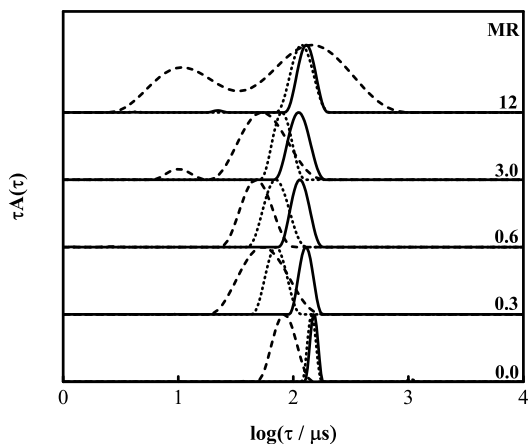
Figure 3.9. Comparison of relaxation time distributions of three PEO-PPO-PEO block copolymer-bile salt mixed systems at 50 °C and at different MR. F127-NaGDC system (solid line), P123-NaGDC system (dotted line), and P65-NaGDC system (dashed line). The copolymer concentration was 1.0 wt %.

3.1.6. Complex Structure and Interactions in the F127- or P65-NaGDC Systems (Paper I and III)

The obtained $p(r)$ functions from the IFT analysis of the SAXS data for the mixed P65-NaGDC and F127-NaGDC systems at 50 °C demonstrated a decrease in the radii of the complexes by addition of NaGDC, as previously seen for the P123-NaGDC system (Figure 5 in **Paper III** and Figure 7b in **Paper I**). Up to MR=0.6 the scattering curves of the P65-NaGDC systems were fitted with the analytical spherical core-shell model as a form factor and the Hayter-Penfold model as a structure factor, except for MR=0 where the Percus-Yevick model was used.[61] This model-based data analysis indicated that pure P65 micelles with a spherical core-shell structure that interact as hard spheres were present in the solution (Figure 3.10). As in the P123 case (section 3.1.3), the core of the P65 micelle was assumed in the calculations to consist of mostly water and PPO, and the shell mostly of water and PEO. The formation of charged P65 micelle-NaGDC complexes up to MR=0.6 was mirrored in the scattering curves. As noticed, there was a decrease in the size compared to the P65 micelle where both core and shell decreased in size due to accommodation of the bile salt. In addition, the repulsive intercomplex interactions increased as bile salt was added

to the system. The change in the scattering length density of the core was negligible compared to that for pure micelles (MR=0), which clearly demonstrated that NaGDC with a high scattering length density could not be in the core. Nevertheless, the increase in the scattering length density of the shell by addition of NaGDC suggested that the NaGDC monomers were located in the shell close to the core-corona interface (Table S6 in SI, **Paper III**).
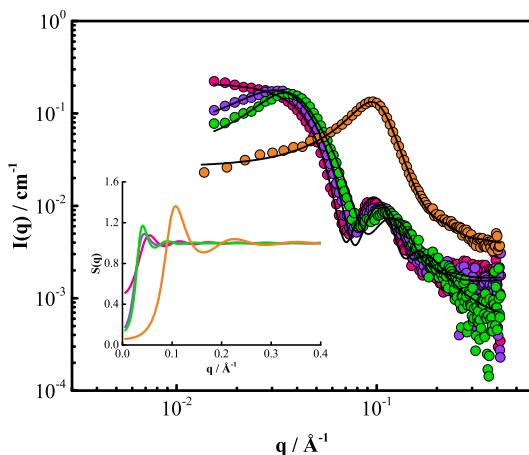
Figure 3.10. P65-NaGDC system; SAXS curves for a 5.0 wt % P65 solution at various MR at 50 °C (symbols); MR=0 (pink), MR=0.3 (violet), MR=0.6 (green) and MR=12 (orange). The solid lines corresponded the fitted curves. The inset shows the analysed structure factors $S(q)$ based on the Percus-Yevick (MR=0) and Hayter-Penfold (MR=0.3-12) method (same color code used).

At MR=3, as a consequence of the break-up of the complexes under which they coexist with small NaGDC-rich complexes, there was an increase in the polydispersity of the system, and the corresponding scattering curve could not be fitted. However at MR=12, where a majority of the complexes were in the form of NaGDC-rich complexes, the scattering curve could only be fitted with a formation of the homogeneous sphere model. These small complexes were interacting with each other via a strong repulsive interparticle interaction of charged hard spheres, and a structure factor calculated with the Hayter-Penfold method was employed. The size of these complexes (R=2.0 nm) was comparable to the size of the pure NaGDC micelles (R=2.0 nm) at 40 °C.

Analysis of the SAXS scattering curves of the pure P65 and F127 micelles at 20 °C, which was below their corresponding CMT, revealed that unassociated block copolymers existed as Gaussian chains in the solutions, with gyration radii (R_g) of 2.2 and 2.1 nm respectively (Figure 7 in **Paper III**). In the P123 case, 20 °C was above the CMT and thus, the P123 block copolymers were associated in the form of spherical core-shell micelles (Figure 3.11). At MR=12, however, all scattering curves resembled that of a NaGDC micelle in 200 mM solution (Figure

7 in **Paper III**). The obtained radii were 2.0, 1.8, and 1.8 nm for P123, F127, and P65, respectively. These values were comparable to the size of the pure NaGDC micelle. Due to the lower concentrations of NaGDC in the mixed solutions, and consequently smaller repulsive interactions compared to the pure NaGDC solution, the scattering curves of P123 and F127 at MR=12 did not completely overlap with that of the pure NaGDC solution. However, in the case of P65 and at MR=12 where the concentration of NaGDC (176 mM) was close to that of the pure NaGDC solution, the scattering curves were very similar. These SAXS results together with the presence of a small endothermic hump in the DSC data at 20 °C (Figure S3 in SI, **Paper III**) suggested that NaGDC micelles interact with unimers below the CMT of the block copolymer. It also reinforced the hypothesis that the same types of complexes form when block copolymer micelles are disintegrated by NaGDC at temperatures well above the CMT. The formation of these small NaGDC-rich complexes at low temperature prevents formation of larger PEO-PPO-PEO micelle-NaGDC complexes upon temperature increase, and thus the CMT of the block copolymer increases.
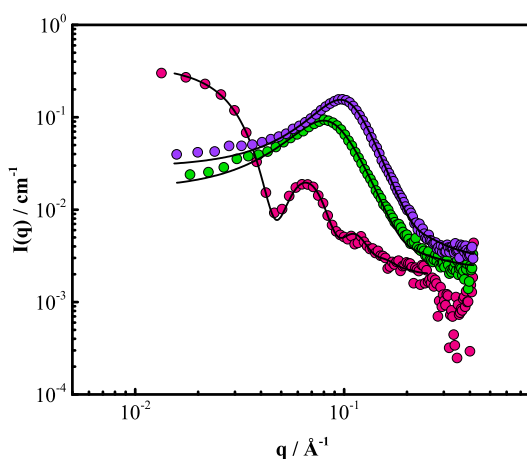
Figure 3.11. SAXS curves for 5.0 wt % P123 solutions at various MR at 20 °C (symbols); MR=0 (pink) and MR=12 (green). Also shown is a 200 mM NaGDC aqueous solution (violet). The solid lines corresponded the fitted curves.

Part II

3.2. Charged PNIPAAM Diblock Copolymers and Their Mixtures in Aqueous Solution

A thermoresponsive polymer like PNIPAAM, which has a phase transition close to body temperature, is an attractive polymer for drug delivery applications. To improve the performance of using PNIPAAM for this purpose, tuning the phase

behavior of PNIPAAM in aqueous solution may be done by synthesizing block copolymers based on PNIPAAM. The attributes of the attached block can then make the PNIPAAM suitable for the desired applications. Studies of these polymer systems are valuable from a fundamental scientific perspective in order to understand their potential to be used for instance in pharmaceutical applications.

In this part of the thesis, as a first step, methods such as DLS and turbidymetry were used to investigate the effects of temperature, block copolymer concentration, length of the PNIPAAM block, and salt on the association behavior of the series of cationic diblock copolymers poly(N-isopropylacrylamide)-b-poly((3-acrylamidopropyl) trimethylammonium chloride) or PNIPAAM$_n$-b-PAMPTMA(+)$_{20}$, with n=24, 48, and 65.

In the next step, a cationic diblock copolymer of PAMPTMA(+), with approximately the same block length as the one with the shortest PNIPAAM block length used in **Paper IV**, was mixed with its anionic pair with a constant 1:1 molar charge ratio. The aim was to investigate the formation of mixed micelles, which was driven by the electrostatic interaction between the charged blocks of the copolymers. The effects of temperature and total concentration of the mixed solution on the association behavior of these mixed micelles were studied by DLS and SLS, SAXS, turbidimetry, HSDSC, 2D ^{1}H NMR NOESY, and electrophoretic mobility measurements (**Paper V**).

3.2.1. Effects of Temperature and Salt Addition on the Association Behavior of Cationic PNIPAAM Diblock Copolymers (Paper IV)

It was observed both visually and by turbidity measurements that an increase in temperature caused an augmentation of the turbidity in the PNIPAAM$_n$-b-PAMPTMA(+)$_{20}$ block copolymer solutions, due to the formation of aggregates as a result of the increase in hydrophobicity of PNIPAAM with temperature (Figure 5 in **Paper IV**). At a constant concentration, the block copolymers with a longer PNIPAAM block thus demonstrated an increase in turbidity at lower temperatures. The investigation of the cloud points clearly illustrated that for an individual block copolymer, the more concentrated solutions had lower CP due to the higher collision frequency of the hydrophobic parts as the temperature increased. This effect was more pronounced for the block copolymer with the shortest PNIPAAM block (n=24). The effect of salt (NaCl) addition to the block copolymer solution with the longest PNIPAAM block (n=65) caused a suppression of the CP as the salt concentration increased. This feature was evidently due to screening of the repulsive electrostatic interactions between the polymers/aggregates (Figure 3.12).
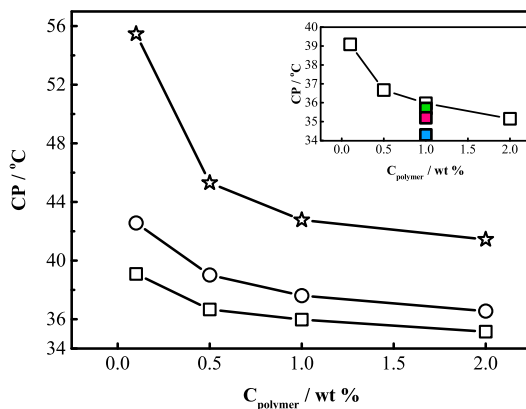
Figure 3.12. Effect of polymer concentration and PNIPAAM block length on the cloud point (CP) of aqueous solutions of $PNIPAAM_n$-b-$PAMPTMA(+)_{20}$ with n=24 (star symbol), n=48 (circle symbol) and n=65 (square symbol). Inset demonstrates effect of 0.01 M (green symbol), 0.05 M (red symbol) and 0.1 M (blue symbol) NaCl addition on the cloud point of the block copolymer with n=65.

Zeta potential measurements demonstrated that for all three block copolymers, the charge density increased at the elevated temperatures. This result indicated that the charged blocks built up the corona of the particles and the PNIPAAM blocks were located mostly in the core. Moreover, due to the compaction of the PNIPAAM blocks as the temperature increased, the charged moieties of the block copolymers were forced out to the surface of the particles. Due to the increase in hydrophobicity, this effect was more noticeable for the block copolymer with the longer PNIPAAM block.

For all block copolymers, the intensity correlation functions obtained from DLS were biexponential and revealed the coexistence of unimers (corresponding to the fast relaxation time) and aggregates (corresponding to the slow relaxation time) at temperatures well below the cloud point. The apparent hydrodynamic radius of the unimers was obviously larger for the copolymers with a longer PNIPAAM block (Figure 8a in **Paper IV**).

The clusters on the other hand shrunk in size at temperatures below the cloud point while they grew in size at higher temperatures due to the formation of larger aggregates. The polymer with the longest PNIPAAM chain showed these features more significantly (Figure 3.13). Although the aggregate size of the two block copolymers with longer PNIPAAM chains was comparable at higher temperatures, the reduced scattering intensity indicated that the clusters of the block copolymer with a longer PNIPAAM block were more compact than those with shorter blocks.

Figure 3.13. Temperature dependence of the clusters apparent hydrodynamic radius (slow mode) for a 1 wt % aqueous solutions of PNIPAAM$_n$-b-PAMPTMA(+)$_{20}$ with n=24 (star symbol), n=48 (circle symbol) and n=65 (square symbol).

As mentioned, addition of NaCl to the 1 wt % solution of the block copolymer with n=65 indicated that there was a screening of repulsive electrostatic interactions in the system. At temperatures well below the CP, there was a decrease in the cluster size in the order of increasing salt concentration due to compaction of the clusters (Figure 3.14). At the elevated temperature above the CP however, a small addition of salt (0.01 M) caused a compaction of the aggregates while a larger addition (0.1 M) instead induced an aggregate growth. Moreover, the stability (in terms of size) of the aggregates improved at intermediate salt concentrations.

The electric field correlation functions were fitted to a biexponential function with stretched exponents (see eq. (15) in section 2.1.1). The values of the stretched exponents related to the aggregates, approached unity at elevated temperatures for solutions both with and without salt. This suggested that the polydispersity of the aggregates became smaller with increasing temperature and can be attributed to the Ostwald ripening phenomena where the larger particles become larger and the smaller ones disappear.
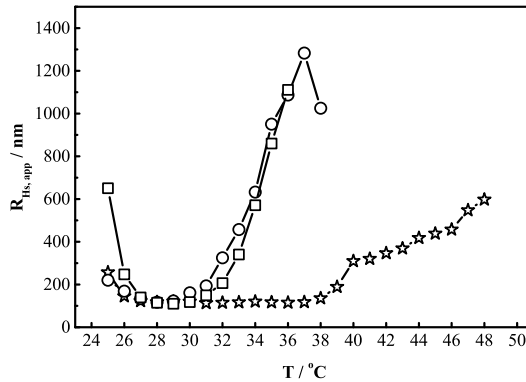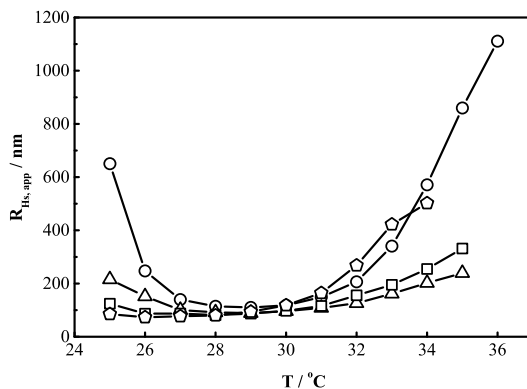
Figure 3.14. Effect of NaCl addition on Temperature dependence of the clusters apparent hydrodynamic radius (slow mode) for a 1 wt % aqueous solutions of PNIPAAM$_n$-*b*-PAMPTMA(+)$_{20}$ with n=65. Solutions without salt and with 0.01 M, 0.05 M, and 0.1 M were represented by circle, triangle, square and pentagon symbols respectively.

3.2.2. Mixed Micelles of Oppositely Charged PNIPAAM Diblock Copolymers (Paper V)

The DLS measurements on the mixed solutions of PNIPAAM$_{26}$-*b*-PAMPTMA(+)$_{15}$ and poly(*N*-isopropylacrylamide)-*b*-poly(sodium 2-acrylamido-2-methyl-1-propanesulfonate) or PNIPAAM$_{27}$-*b*-PAMPS($-$)$_{15}$ (charge molar ratio $n_+/n_- = 1$) demonstrated the presence of mixed micelles in the concentration range of 0.2–0.5 wt % and at all studied temperatures (10–30 ^{o}C) (Figure 3.15). $R_{H,app}$ of the mixed micelles for the 0.2 wt % solution at 15 ^{o}C was about 8.41 nm, which did not change significantly with increased concentration at this temperature. However, a slight growth of the mixed micelles at temperatures above 15 ^{o}C for 0.2–0.5 wt % solutions was attributed to an increase in the aggregation number of mixed micelles (Figure 7a in **Paper V**).

The SAXS data analysis of the mixed 0.2 wt % solution at a temperature range of 10–34 ^{o}C revealed that the mixed micelles have a cylindrical structure (Table S1 in SI, **Paper V** and Figure 3.16). From the length and the radius of the cylinder obtained from the fits of the SAXS data, a theoretical value of the hydrodynamic radius for a rod was estimated, which agreed well with the experimental value.

The electrophoretic mobility measurement on the same sample at 15 ^{o}C confirmed that the mixed micelles were charge neutral, which indicated that they were formed by electrostatic interactions between the charged blocks (PAMPTMA(+)$_{15}$ and PAMPS($-$)$_{15}$). The 2D ^{1}H NMR NOESY experiment on the same solution and temperature revealed that although there was strong evidence of close proximity of the charged blocks in the mixed micelles, there

was also a possibility for interaction between PNIPAAM and the charged blocks (which could be either inter- or intramolecular nature). Hence, there is not a strong segregation between the PNIPAAM and charged blocks in the mixed micelles, instead some block mixing occurred (Figure 3 and 4 in **Paper V**).
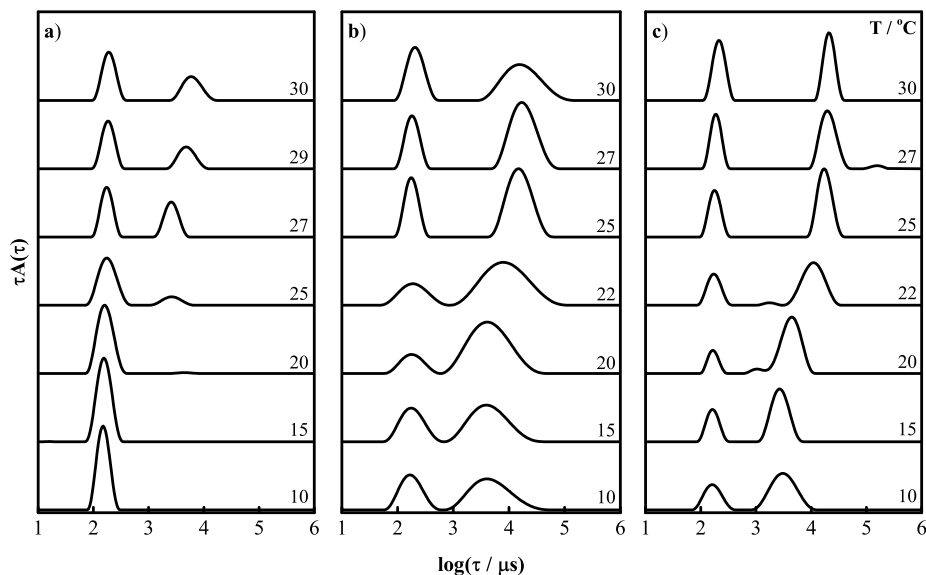
Figure 3.15. Relaxation time distributions at different temperatures of mixed block copolymer solutions with $c_{polymer}$ equal to a) 0.2 wt %, b) 0.3 wt % and c) 0.5 wt %.

For the mixed 0.3–0.5 wt % solutions in the temperature range of 10–30 °C and for the 0.2 wt % solution above 20 °C, the DLS data demonstrated coexistence of the mixed micelles with the larger aggregates or clusters that grew in size upon increased temperature (Figure 7 in **Paper V** and Figure 3.15). The turbidity rose above the CP of the mixed solutions and caused a further growth of these clusters. The results from the measurements on the same solutions confirmed that in the concentration range of 0.2–1 wt % the cloud points of mixed solutions were not concentration dependent, and that the values of the endothermic transition enthalpies per mole of NIPAAM unit were very close to that of the pure PNIPAAM$_{30}$ solution (Figure 2 and Table 1 in **Paper V**). Keeping in mind the previously reported temperature behavior of PNIPAAM homopolymers,[35, 62] these values suggested that the formation of the large aggregates was related to intermicellar aggregation via the hydrophobic interaction between the dehydrated PNIPAAM blocks of the micellar corona.

Figure 3.16. SAXS curves (symbols) at different temperatures with corresponding curves from fitting (solid lines) of an aqueous solution containing mixed micelles of PNIPAAM$_{26}$-*b*-PAMPTMA(+)$_{15}$ and PNIPAAM$_{27}$-*b*-PAMPS($-$)$_{15}$. Temperatures: 10 °C (red), 15 °C (black), 20 °C (violet), 25 °C (orange), 30 °C (green), 32 °C (pink), 34 °C (blue). $c_{polymer}$ was 0.2 wt %.
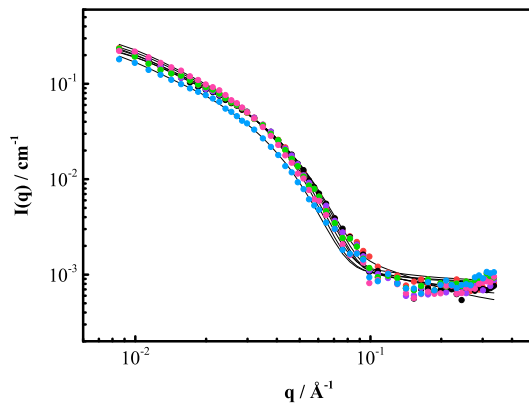
4

Conclusions and Future Remarks

In this thesis, two types of thermoresponsive amphiphilic block copolymers were investigated in aqueous solution; PEO-PPO-PEO triblock copolymers and charged diblock copolymers containing a PNIPAAM block. The first part of the thesis was dedicated to understand the effect of a bile salt, NaGDC, on the self-association of the three PEO-PPO-PEO block copolymers P123, F127, and P65. P65 and F127 have either the same length of PEO or PPO block compared to P123. The overall aim was to investigate the potential use of these types of polymers as bile salt carriers in the treatment of *bile acid diarrhea* and *hypercholesterolemia* diseases. It was found that NaGDC, the biological surfactant, can influence the block copolymer self-assembly in a similar way as conventional ionic surfactants. However, due to its particular structure and characteristics, NaGDC is generally a ''weaker'' surfactant in terms of ability to disintegrate the PEO-PPO-PEO micelles. Depending on the type of copolymer and on the NaGDC concentration, two types of complexes can be observed at temperatures well above the CMT of the pure polymers. At low concentration of NaGDC, charged PEO-PPO-PEO micelle-NaGDC complexes are formed. It was also found that the block copolymer micelles accommodate the NaGDC monomers mostly in their corona yet closer to the core-corona interface. At higher NaGDC concentrations, the bile salt starts to disintegrate these complexes by peeling off unimers and forming a second type of complexes, which resemble the NaGDC micelles in size. It was shown by a simple stoichiometric DSC model that they contain one or few PEO-PPO-PEO unimers. The two complexes mentioned above coexist up to the highest NaGDC concentration investigated in this study. It is expected that at very high NaGDC concentrations, the NaGDC-rich complexes are the dominant species in the solution and the block copolymer micelles are completely broken up (not covered in this study). The P65 micelle was found to be the one most easily disintegrated by NaGDC among the three PEO-PPO-PEO micelles while the effect of NaGDC on the disintegration of F127 and P123 micelles was moderate. This shows that both the PPO block length and the molecular weight in addition to PPO/PEO composition ratio

determines the ability of the bile salt to break up the micelles. From these findings, it can be concluded that due to the lower stability of its micelle when in contact with NaGDC, the P65 block copolymer is not a good candidate to be used as a bile salt carrier compared to P123 and F127. On the other hand both F127 and P123 micelles seem to be good candidates for such an application, but to draw a better conclusion, the effect of other parameters such as physiological conditions and other bile salts on their self-assembly behavior have to be investigated.

In the second part of this thesis, a series of another type of amphiphilic and thermoresponsive block copolymers in aqueous solutions were studied, namely PNIPAAM$_n$-b-PAMPTMA(+)$_{20}$ with three different PNIPAAM block lengths. It was discovered that the cloud point in all three block copolymers decreases with increased polymer concentration and increased PNIPAAM block lengths as well as by addition of salt. At temperatures well below the CP, two types of species coexist in the block copolymer solutions: block copolymer unimers and clusters. These clusters grow in size, depending on the PNIPAAM block length, and become the dominant species in the solution at temperatures close to the CP of the solutions. Above CP the apparent hydrodynamic size of the clusters decreases by a small addition of salt due to the screening of the electrostatic repulsive interactions. Generally, in the presence of salt the clusters were more stable in terms of size upon increasing temperature.

Lastly, the influence of temperature and concentration on the behavior of mixed aqueous solutions of cationic PNIPAAM$_{26}$-b-PAMPTMA(+)$_{15}$ and its anionic pair diblock copolymer PNIPAAM$_{27}$-PAMPS(−)$_{20,}$ with a mixing charge ratio of 1:1 was studied. The results at 10 ^{o}C demonstrated the presence of mixed micelles with an apparent hydrodynamic radius of 8–9 nm. The mixed micelles are charge neutral and their formation was driven by an attractive electrostatic interaction between the oppositely charged blocks. The 2D ^{1}H NMR NOESY measurements gave direct evidence that the charged blocks form the core of the mixed micelles whereas the PNIPAAM blocks were mostly present in the corona. At higher concentrations, mixed micelles were in coexistence with larger-sized clusters. The mixed micelles have a cylindrical structure according to SAXS measurements, with a radius of about 3 nm and the length of about 35 nm. For all concentrations, the size of the mixed micelles was found to increase by temperature as a reflection of an increase in molecular weight of the micelles. The formation of clusters at the temperatures below the CP might be due to the weak hydrophobic interaction of PNIPAAM segments in the block copolymers and/or associated to the formation of intermicellar aggregates. The growth of these clusters by temperature is attributed to the dehydration of the PNIPAAM block and formation of intermicellar aggregates at temperatures above the CP.

All amphiphilic block copolymers that were studied in this thesis are thermoresponsive. At temperatures close to body temperature, all are either in the form of micelles and/or intermicellar aggregates. In addition, due to the low toxicity of these polymers, micelles of these block copolymers could be considered to be structures well-suited for drug delivery applications. It was shown how parameters such as the hydrophobic/hydrophilic balance, concentration, salt and natural ionic surfactant addition, temperature, and molecular weight can influence the self-assembly of these polymers. Knowledge of the self-association behavior of these block copolymers under the influence of these parameters in addition to others not covered in this thesis could empower us to tune the block copolymer characteristics for the desired application. Forming mixed micelles of these block copolymers opens doors to other applications that need multi-functional micelles for multi-purpose applications. It is worth mentioning that in line with the aim of the present investigations about the specific applications of PEO-PPO-PEO block copolymers as bile acid sequestrants, currently the effects of bile salts on the self-assembly of the cationic PNIPAAM-based block copolymers are studied. Even if in future it becomes evident that the polymers studied in this thesis are not appropriate for this specific aim of bile acid sequestrants, still understanding the effect of natural surfactants such as bile salts on the self-assembly of these block copolymers may lead us to use the mixed micelles or complexes of bile salts and block copolymers in drug delivery applications with a different goal.

References

1. Riess, G., Micellization of Block Copolymers. *Prog. Polym. Sci.* **2003,** *28*, 1107-1170.

2. Lazzari, M.; Liu, G.; Lecommandoux, S., *Block copolymers in nanoscience*. John Wiley & Sons: 2007.

3. Alexandridis, P., Amphiphilic copolymers and their applications. *Curr. Opin. Colloid In.* **1996,** *1*, 490-501.

4. Jones, M.-C.; Leroux, J.-C., Polymeric micelles–a new generation of colloidal drug carriers. *Eur. J. Pharm. Biopharm.* **1999,** *48*, 101-111.

5. Kataoka, K.; Harada, A.; Nagasaki, Y., Block copolymer micelles for drug delivery: design, characterization and biological significance. *Adv. Drug Deliver. Rev.* **2001,** *47*, 113-131.

6. Malmsten, M., In *Amphiphilic Block Copolymers. Self-Assembly and Applications*, Alexandridis, P.; Lindman, B., Eds. Elsevier Science SV: Amsterdam, 2000; p 319.

7. Evans, D. F.; Wennerström, H., *The Colloidal Domain: where Physics, Chemistry, Biology, and Technology Meet*. 2nd ed.; Wiley-VCH: U.S.A., 1999.

8. Loh, W., Block copolymer micelles. *Encyclopedia of surface and colloid science* **2002**, 802-813.

9. Attia, A. B. E.; Ong, Z. Y.; Hedrick, J. L.; Lee, P. P.; Ee, P. L. R.; Hammond, P. T.; Yang, Y.-Y., Mixed micelles self-assembled from block copolymers for drug delivery. *Curr. Opin. Colloid In.* **2011,** *16*, 182-194.

10. Alexandridis, P.; Hatton, T. A., Poly(ethylene oxide)-Poly(propylene oxide)-Poly(ethylene oxide) Block Copolymers Surfactants in Aqueous Solutions and at Interfaces: Thermodynamics, Structure, Dynamics and Modeling. *Colloid. Surface. A* **1995,** *96*, 1-46.

11.   Batrakova, E. V.; Kabanov, A. V., Pluronic Block Copolymers: Evolution of Drug Delivery Concept from Inert Nanocarriers to Biological Response Modifiers. *J. Control Release* **2008,** *130*, 98–106.

12.   Karlström, G., A New Model for Upper and Lower Critical Solution Temperatures in Poly(ethylene oxide) Solutions. *J. Phys. Chem.* **1985,** *89*, 4962-4964.

13.   Lindman, B.; Medronho, B.; Karlström, G., Clouding of nonionic surfactants. *Curr. Opin. Colloid In.* **2016,** *22*, 23-29.

14.   Linse, P., Micellization of Poly(ethylene oxide)-Poly(propylene oxide) Block Copolymers in Aqueous Solution. *Macromolecules* **1993,** *26*, 4437-4449.

15.   Alexandridis, P.; Holzwarth, J. F.; Hatton, T. A., Micellization of poly (ethylene oxide)-poly (propylene oxide)-poly (ethylene oxide) triblock copolymers in aqueous solutions: thermodynamics of copolymer association. *Macromolecules* **1994,** *27*, 2414-2425.

16.   Wanka, G.; Hoffman, H.; Ulbricht, W., Phase Diagrams and Aggregation Behavior of Poly(oxyethylene)-Poly(oxypropylene)-Poly(oxyethylene) Triblock Copolymers in Aqueous Solutions. *Macromolecules* **1994,** *27*, 4145-4159.

17.   Hvidt, S.; Trandum, C.; Batsberg, W., Effects of poloxamer polydispersity on micellization in water. *J. Colloid Interf. Sci.* **2002,** *250*, 243-250.

18.   Linse, P., Micellization of Poly(ethylene oxide)-Poly(propylene oxide) Block Copolymers in Aqueous Solution: Effect of Polymer Polydispersity. *Macromolecules* **1994,** *27*, 6404-6417.

19.   Mortensen, K.; Batsberg, W.; Hvidt, S., Effects of PEO-PPO diblock impurities on the cubic structure of aqueous PEO-PPO-PEO pluronics micelles: fcc and bcc ordered structures in F127. *Macromolecules* **2008,** *41*, 1720-1727.

20.   Brown, W.; Schillén, K.; Almgren, M.; Hvidt, S.; Bahadur, P., Micelle and Gel Formation in a Poly(ethylene oxide)-Poly(propylene oxide)-Poly(ethylene oxide) Triblock Copolymer in Water Solution. Dynamic and Static Light Scattering and Oscillatory Shear Measurements. *J. Phys. Chem.* **1991,** *95*, 1850-1858.

21.   Manet, S.; Lecchi, A.; Imperor-Clerc, M.; Zholobenko, V.; Durand, D.; Oliveira, C. L. P.; Pedersen, J. S.; Grillo, I.; Meneau, F.; Rochas, C., Structure of

Micelles of a Nonionic Block Copolymer Determined by SANS and SAXS. *J. Phys. Chem. B* **2011,** *115*, 11318–11329.

22.   Mortensen, K.; Pedersen, J. S., Structural Study on the Micelle Formation of Poly(ethylene oxide)-Poly(propylene oxide)-Poly(ethylene oxide) Triblock Copolymer in Aqueous Solution. *Macromolecules* **1993,** *26*, 805–812.

23.   Jørgensen, E. B.; Hvidt, S.; Brown, W.; Schillen, K., Effects of salts on the micellization and gelation of a triblock copolymer studied by rheology and light scattering. *Macromolecules* **1997,** *30*, 2355-2364.

24.   Löf, D.; Niemiec, A.; Schillén, K.; Loh, W.; Olofsson, G., A Calorimetry and Light Scattering Study of the Formation and Shape Transition of Mixed Micelles of $EO_{20}PO_{68}EO_{20}$ Triblock Copolymer (P123) and Nonionic Surfactant ($C_{12}EO_6$). *J. Phys. Chem. B* **2007,** *111*, 5911-5920.

25.   Schillén, K.; Brown, W.; Johnsen, R. M., Micellar Sphere-to-Rod Transition in an Aqueous Triblock Copolymer System. A Dynamic Light Scattering Study of Translational and Rotational Diffusion. *Macromolecules* **1994,** *27*, 4825-4832.

26.   Almgren, M.; van Stam, J.; Lindblad, C.; Li, P.; Stilbs, P.; Bahadur, P., Aggregation of Poly(ethylene oxide)-Poly(propylene oxide)-Poly(ethylene oxide) Triblock Copolymers in the Presence of Sodium Dodecyl Sulfate in Aqueous Solution. *J. Phys. Chem.* **1991,** *95*, 5677–5684.

27.   da Silva, R. C.; Olofsson, G.; Schillén, K.; Loh, W., Influence of Ionic Surfactants on the Aggregation of Poly(ethylene oxide)-Poly(propylene oxide)-Poly(ethylene oxide) Block Copolymers Studied by Differential Scanning and Isothermal Titration Calorimetry. *J. Phys. Chem. B* **2002,** *106*, 1239-1246.

28.   Hecht, E.; Hoffmann, H., Interaction of ABA Block Copolymers with Ionic Surfactants in Aqeuous Solution. *Langmuir* **1994,** *10*, 86-91.

29.   Jansson, J.; Schillén, K.; Olofsson, G.; da Silva, R. C.; Loh, W., The Interaction between PEO-PPO-PEO Triblock Copolymers and Ionic Surfactants in Aqueous Solution Studied using Light Scattering and Calorimetry. *J. Phys. Chem. B* **2004,** *108*, 82-92.

30.   Li, Y.; Xu, R.; Coudrec, S.; Bloor, D. M.; Holzwarth, J. F.; Wyn-Jones, E., Binding of Tetradecyltrimethylammonium Bromide to the ABA Block Copolymer Pluronic F127 ($EO_{97}PO_{69}EO_{97}$): Electromotive Force, Microcalorimetry, and Light Scattering Studies. *Langmuir* **2001,** *17*, 5742-4747.

31. Roux, A. H.; Douhéret, G.; Roux-Desgranges, G., Molar Volumes and Isentropic Compressions of Pluronics L64 and P123 in Aqueous Surfactant Solutions, over the Critical Temperature Range of Aggregation. *Colloids Surf. A* **2005,** *252*, 43-50.

32. Thurn, T.; Coudrec, S.; Sidhu, J.; Bloor, D. M.; Penfold, J.; Holzwarth, J. F.; Wyn-Jones, E., Study of Mixed Micelles and Interaction Parameters for ABA Triblock Copolymers of the type EO_m-PO_n-EO_m and Ionic Surfactants: Equilibrium and Structure. *Langmuir* **2002,** *18*, 9267-9275.

33. Schild, H. G., Poly (*N*-isopropylacrylamide): experiment, theory and application. *Prog. Polym. Sci.* **1992,** *17*, 163-249.

34. Alaghemandi, M.; Spohr, E., Macromol. Theory Simul. 2/2012. *Macromo. Theor. Simul.* **2012,** *21* (2).

35. Pamies, R.; Zhu, K.; Kjøniksen, A.-L.; Nyström, B., Thermal response of low molecular weight poly-(*N*-isopropylacrylamide) polymers in aqueous solution. *Polym. Bull.* **2009,** *62*, 487-502.

36. Wei, H.; Cheng, S.-X.; Zhang, X.-Z.; Zhuo, R.-X., Thermo-sensitive polymeric micelles based on poly (*N*-isopropylacrylamide) as drug carriers. *Prog. Polym. Sci.* **2009,** *34*, 893-910.

37. Hofmann, A. F.; Mysels, K., Bile Salts as Biological Surfactants. *Colloids Surf.* **1987,** *30*, 145-173.

38. Madenci, D.; Egelhaaf, S. U., Self-Assembly in Aqueous Bile Salt Solutions. *Curr. Opin. Colloid In.* **2010,** *15*, 109–115.

39. Zarras, P.; Vol, O., Polycationic Salts as Bile Acid Sequestering Agents. *Prog. Polym. Sci.* **1999,** *24*, 485-516.

40. Galantini, L.; di Gregorio, M. C.; Gubitosi, M.; Travaglini, L.; Tato, J. V.; Jover, A.; Meijide, F.; Soto Tellini, V. H.; Pavel, N. V., Bile Salts and Derivatives: Rigid Unconventional Amphiphiles as Dispersants, Carriers and Superstructure Building Blocks. *Curr. Opin. Colloid In.* **2015,** *20*, 170−182.

41. Pártay, L. B.; Sega, M.; Jedlovszky, P., Morphology of bile salt micelles as studied by computer simulation methods. *Langmuir* **2007,** *23*, 12322-12328.

42. Matsuoka, K.; Maeda, M.; Moroi, Y., Micelle Formation of Sodium Glyco- and Taurocholates and Sodium Glyco- and Taurodeoxycholates and

Solubilization of Cholesterol into Their Micelles. *Colloids Surf. A* **2003,** *32*, 87-95.

43. Cozzolino, S. G., L.; Giglio, E.; Hoffmann, S.; Leggio, C.; Pavel, N. V. , Structure of Sodium Glycodeoxycholate Micellar Aggregates from Small-Angle X-ray Scattering and Light-Scattering Techniques. *J. Phys. Chem. B* **2006,** *110*, 12351-12359.

44. Galantini, L.; Giglio, E.; Leonelli, A.; Pavel, N. V., An Integrated Study of Small-Angle X-ray Scattering and Dynamic Light Scattering on Cylindrical Micelles of Sodium Glycodeoxycholate. *J. Phys. Chem. B* **2004,** *108*, 3078-3085.

45. Lopez, F.; Samseth, J.; Mortensen, K.; Rosenqvist, E.; Rouch, J., Micro- and Macrostructural Studies of Sodium Deoxycholate Micellar Complexes in Aqueous Solutions. *Langmuir* **1996,** *12*, 6188–6196.

46. Schurtenberger, P.; Mazer, N.; Känzig, W., Static and Dynamic Light Scattering Studies of Micellar Growth and Interactions in Bile Salt Solutions. *J. Phys. Chem.* **1983,** *87*, 308-315.

47. Fini, A.; Roda, A., Chemical properties of bile acids. IV. Acidity constants of glycine-conjugated bile acids. *J. Lipid Res.* **1987,** *28*, 755-759.

48. Walters, J. R. F.; Pattni, S. S., Managing Bile Acid Diarrhoea. *Ther. Adv. Gastroenterol.* **2010,** *3*, 349-357.

49. Lindner, P., Scattering Experiments: Experimental Aspects, Initial Data Reduction and Absolute Calibration. In *Neutrons, X-rays and light: scattering methods applied to soft condensed matter*, Zemb, T.; Lindler, P., Eds. Elsevier Science B.V.: Amsterdam, 2002.

50. Pusey, P. N., Introduction to Scattering Experiment. In *Neutrons, X-rays and Light: Scattering Methods Applied to Soft Condensed Matter*, Zemb, T.; Lindner, P., Eds. Elsevier Science B.V.: Amsterdam, 2002.

51. Brown, W., Scattering Methods: A Brief Introduction, Lecture notes. Uppsala university: Sweden, 1994.

52. Schurtenberger, P., Contrast and Contrast Variation in Neutron, X-ray and Light Scattering. In *Neutrons, X-rays and Light: Scattering Methods Applied to Soft Condensed Matter*, Zemb, T.; Lindner, P., Eds. Elsevier Science B.V.: Amsterdam, 2002.

53. Pusey, P. N., Dynamic Light Scattering. In *Neutrons, X-rays and light: scattering methods applied to soft condensed matter*, Zemb, T.; Lindner, P., Eds. Elsevier Science B.V.: Amsterdam, 2002.

54. Siegert, A., Radiation Laboratory report no. 465. *Massachusetts Institute of Technology, Cambridge* **1943**.

55. Jakeš, J., Regularized Positive Exponential Sum (REPES) Program–A Way of Inverting Laplace Transform Data obtained by Dynamic Light Dcattering. *Collect. Czech. Chem. Comm.* **1995,** *60*, 1781-1797.

56. Pedersen, J., Modelling of Small-Angle Scattering Data from Colloids and Polymer Systems. In *Neutrons, X-rays and Light: Scattering Methods Applied to Soft Condensed Matter*, Zemb, T.; Lindler, P., Eds. Amsterdam: North Holland Delta Series: 2002.

57. Olofsson, G.; Wang, G., Isothermal Titration and Temperature Scanning Calorimetric Studies of Polymer-Surfactant Systems. In *Polymer–Surfactant Systems*, Kwak, J. C. T., Ed. Marcel Dekker: New York, 1998.

58. Shvartzman-Cohen, R.; Ren, C.-l.; Szleifer, I.; Yerushalmi-Rozen, R., An Isotopic Effect in Self-Assembly of Amphiphilic Block Copolymers: The Role of Hydrogen Bonds. *Soft Matter* **2009,** *5*, 5003–5011.

59. Hayter, J. H.; Penfold, J., An Analytic Structure Factor for Macroion Solutions. *Mol. Phys.* **1981,** *42*, 109-118.

60. Li, Y.; Xu, R.; Coudrec, S.; Bloor, D. M.; Wyn-Jones, E.; Holzwarth, J. F., The Binding of Sodium Dodecyl Sulfate to the ABA Block Copolymer Pluronic F127 ($EO_{97}PO_{69}EO_{97}$): F127 Aggregation Induced by SDS. *Langmuir* **2001,** *17*, 183-188.

61. Percus, J. K.; Yevick, G. J., Analysis of Classical Statistical Mechanics by means of Collective Coordinates. *Phys. Rev.* **1958,** *110*, 1-13.

62. Lazzara, G.; Olofsson, G.; Alfredsson, V.; Zhu, K.; Nyström, B.; Schillén, K., Temperature-responsive inclusion complex of cationic PNIPAAM diblock copolymer and γ-cyclodextrin. *Soft Matter* **2012**, *8*, 5043-5054.